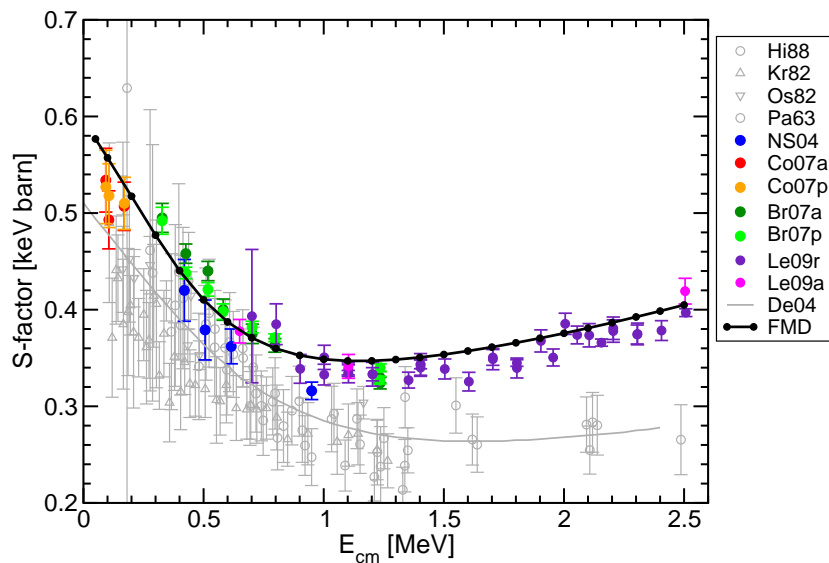


Structure and reactions of light nuclei studied in Fermionic Molecular Dynamics



Thomas Neff
Workshop on
“Limits of existence of Light nuclei”
ECT*, Trento, Italy
Oct 25 - Oct 30, 2010

Overview



Effective Nucleon-Nucleon interaction:

Unitary Correlation Operator Method

- Short-range Correlations
- Correlated Interaction
- *ab initio* Few- and Many-Body Calculations

Many-Body Method:

Fermionic Molecular Dynamics

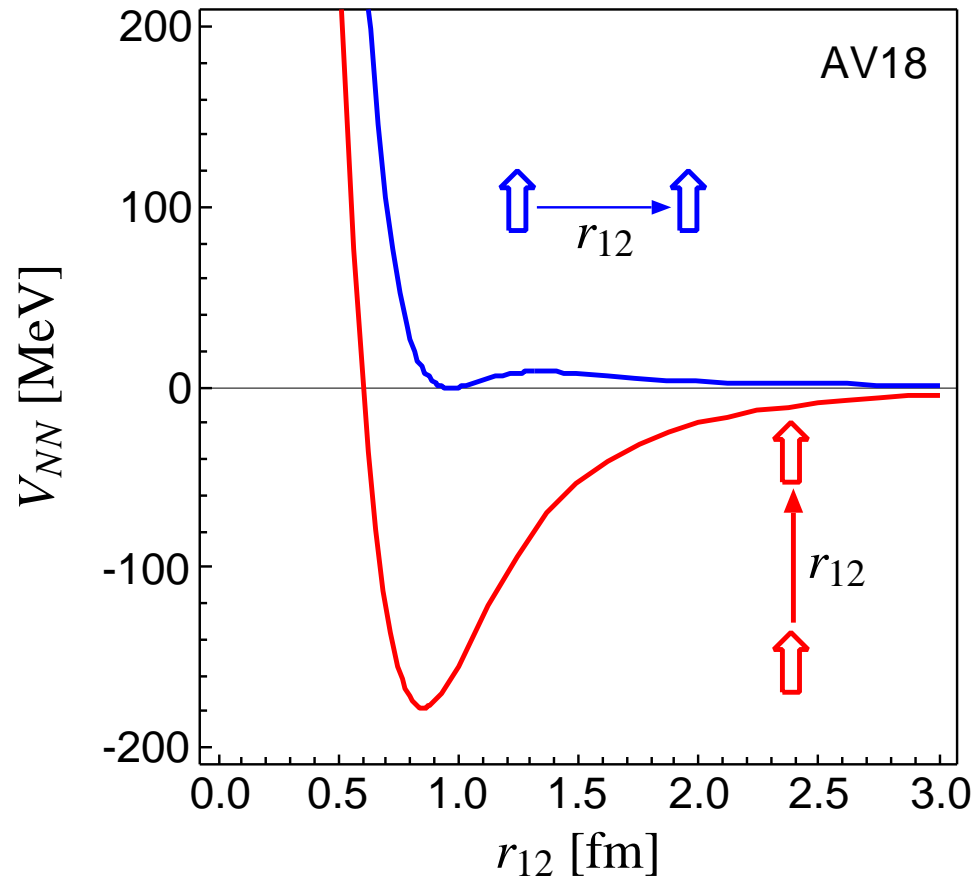
- Model
- Beryllium Isotopes
- Neon Isotopes – Halo-candidate ^{17}Ne
- $^3\text{He}(\alpha, \gamma)^7\text{Be}$ Radiative Capture Reaction

Unitary Correlation Operator Method

Nuclear Force

Argonne V18 (T=0)

spins aligned parallel or perpendicular to the relative distance vector



- strong repulsive core: nucleons can not get closer than ≈ 0.5 fm

➤ **central correlations**

- strong dependence on the orientation of the spins due to the tensor force

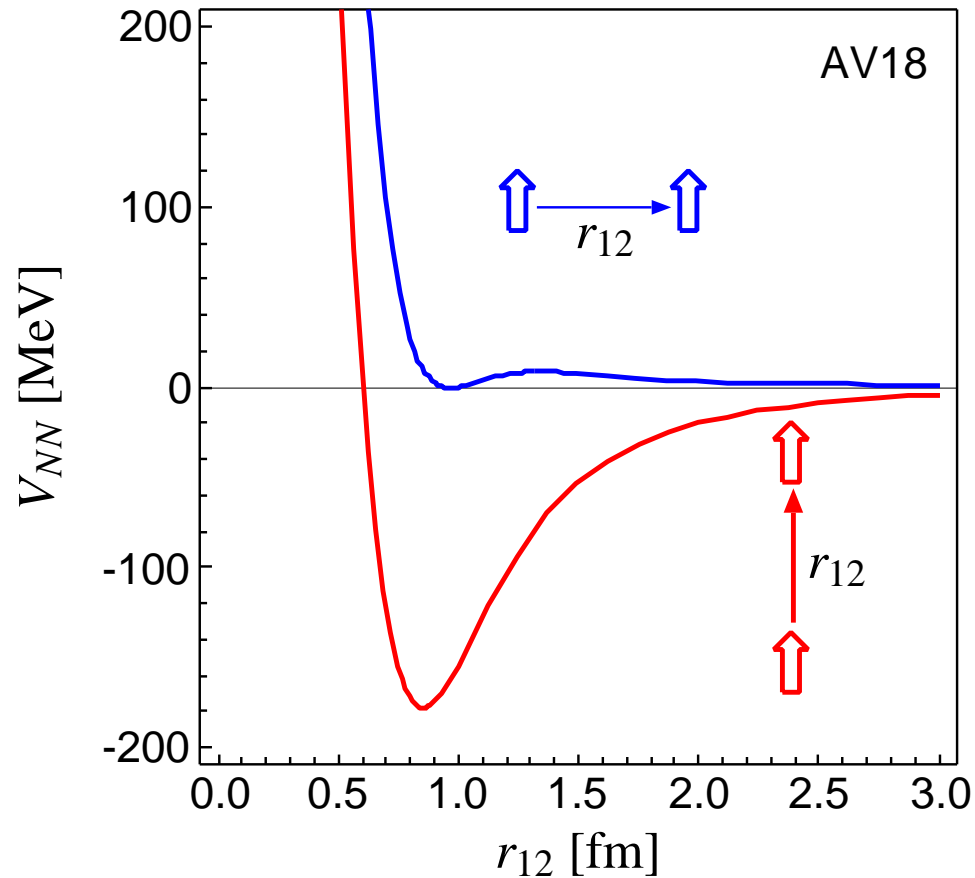
➤ **tensor correlations**

Unitary Correlation Operator Method

Nuclear Force

Argonne V18 (T=0)

spins aligned parallel or perpendicular to the relative distance vector



- strong repulsive core: nucleons can not get closer than ≈ 0.5 fm

➤ **central correlations**

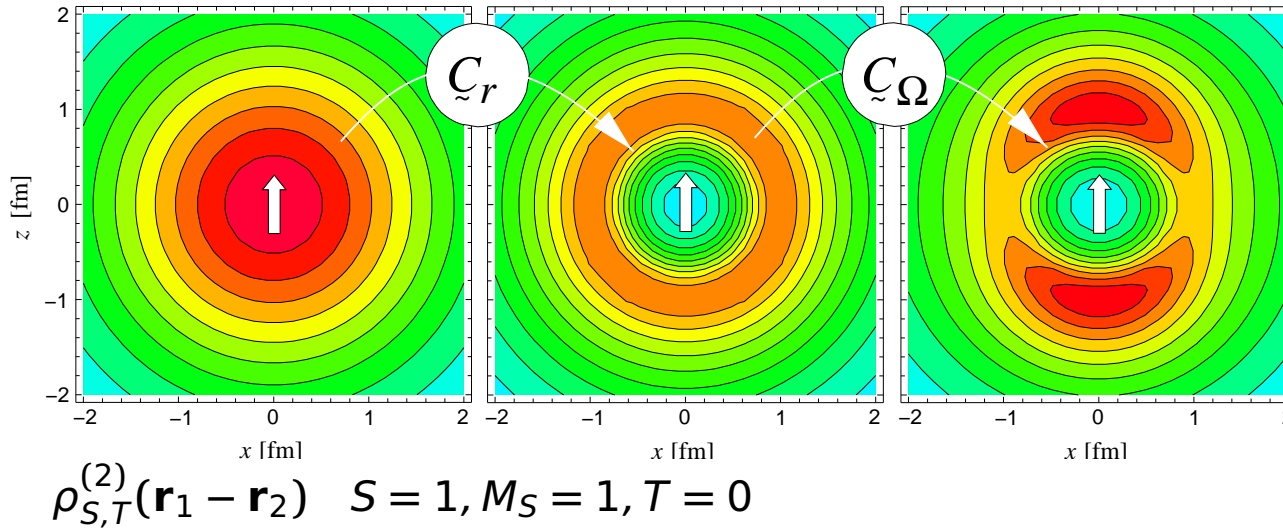
- strong dependence on the orientation of the spins due to the tensor force

➤ **tensor correlations**

the nuclear force will induce **strong short-range correlations** in the nuclear wave function

- Unitary Correlation Operator Method
- Realistic Effective Interaction

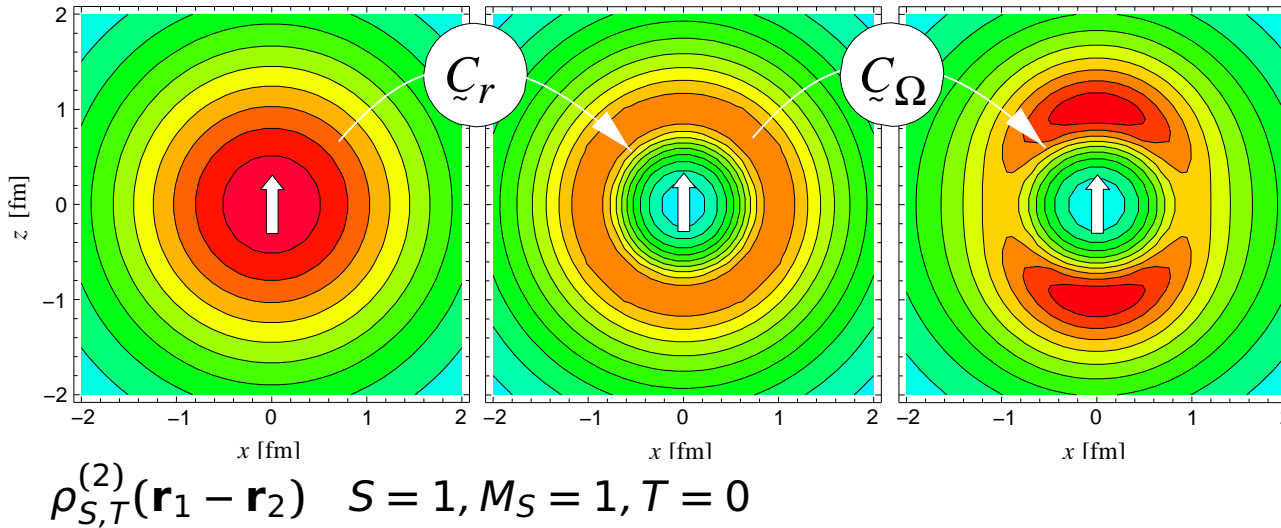
two-body densities



central correlator \tilde{C}_r
 shifts density out of
 the repulsive core
tensor correlator \tilde{C}_Ω
 aligns density with spin
 orientation

Unitary Correlation Operator Method Realistic Effective Interaction

two-body densities

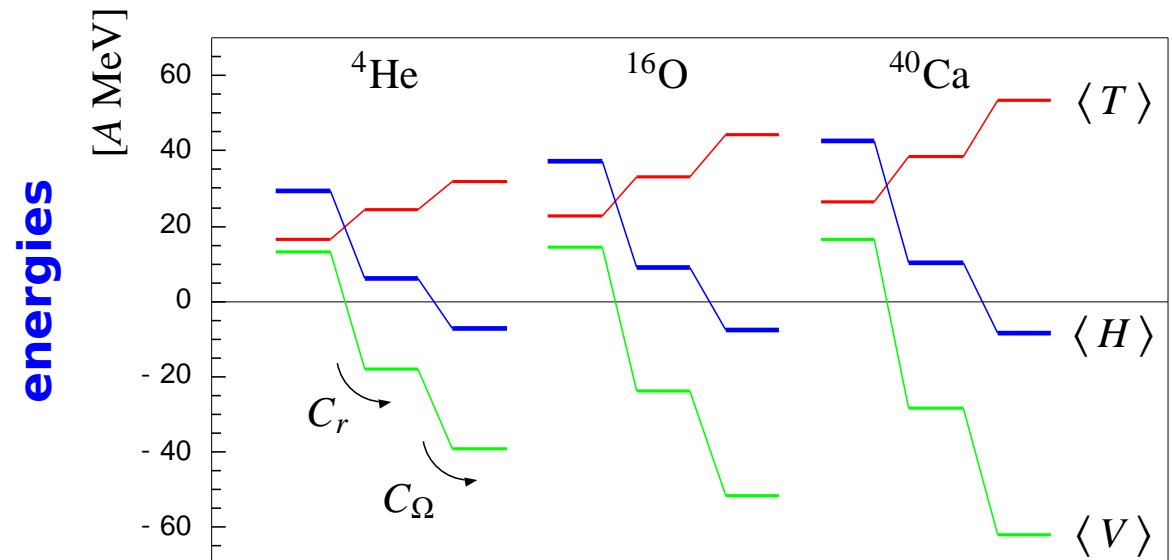


central correlator \tilde{C}_r
shifts density out of
the repulsive core

tensor correlator \tilde{C}_Ω
aligns density with spin
orientation

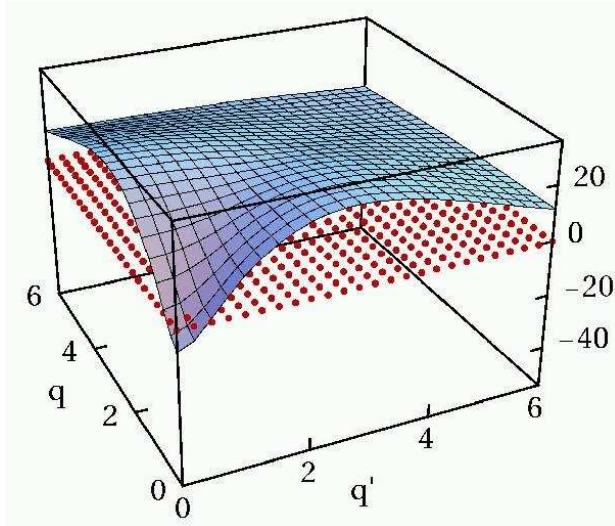
both central
and tensor
correlations are
essential for
binding

$0\hbar\omega$ Harmonic Oscillator



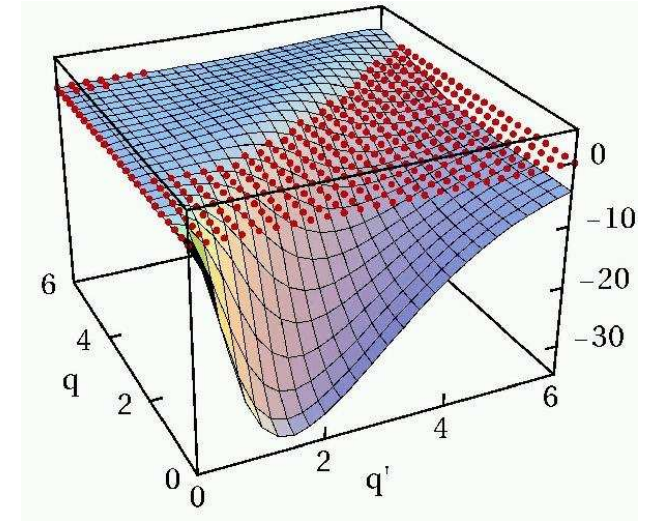
- Unitary Correlation Operator Method
- **Correlated Interaction in Momentum Space**

3S_1 bare



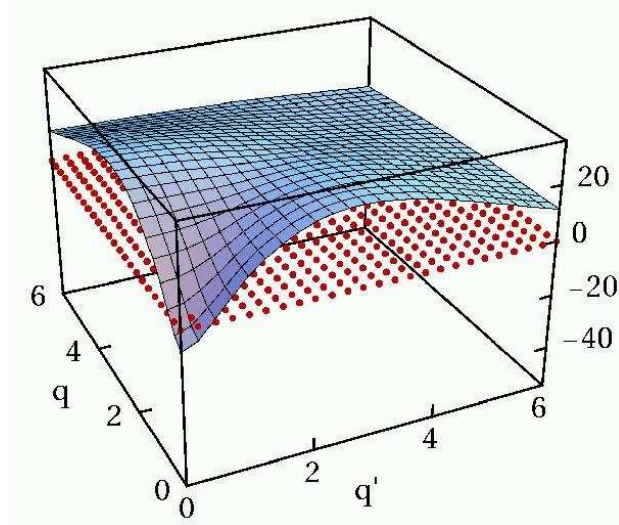
bare interaction has **strong off-diagonal** matrix elements connecting to high momenta

${}^3S_1 - {}^3D_1$ bare



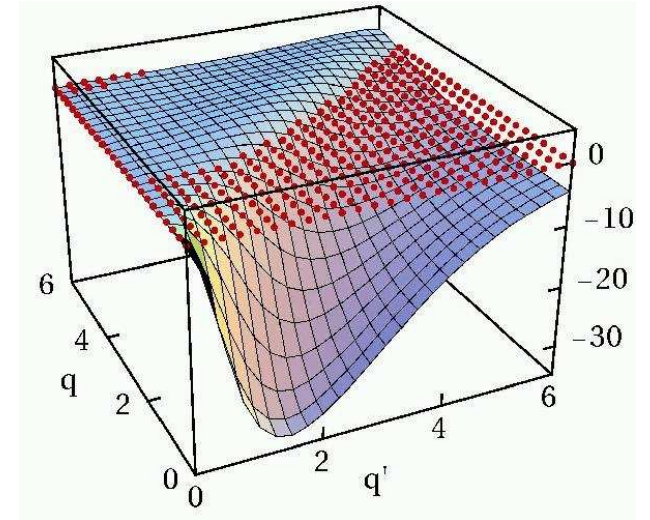
- Unitary Correlation Operator Method
- **Correlated Interaction in Momentum Space**

3S_1 bare



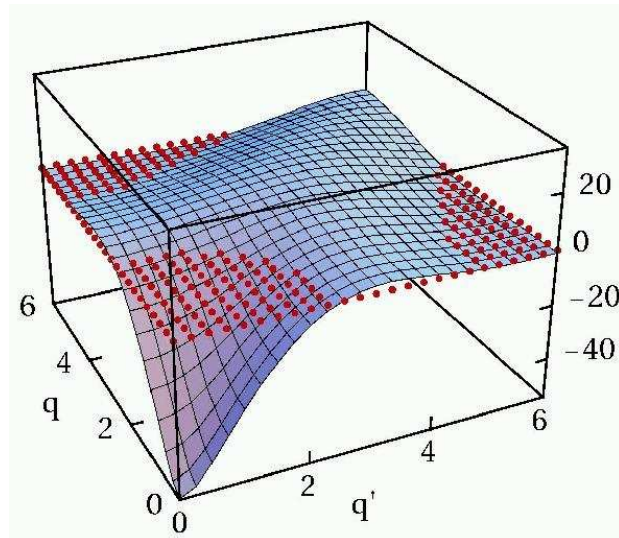
bare interaction has **strong off-diagonal** matrix elements connecting to high momenta

${}^3S_1 - {}^3D_1$ bare



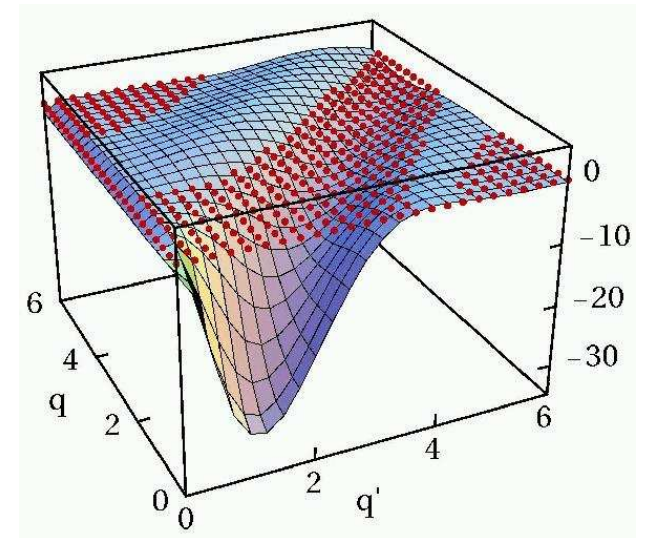
correlated interaction is **more attractive** at low momenta

3S_1 correlated



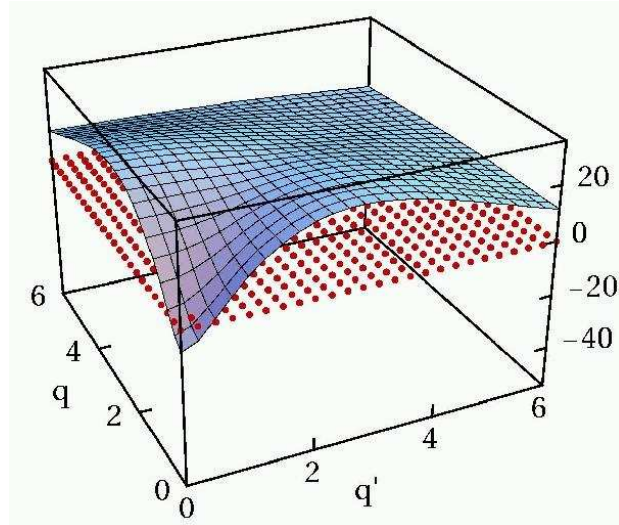
off-diagonal matrix elements connecting low- and high- momentum states are **strongly reduced**

${}^3S_1 - {}^3D_1$ correlated



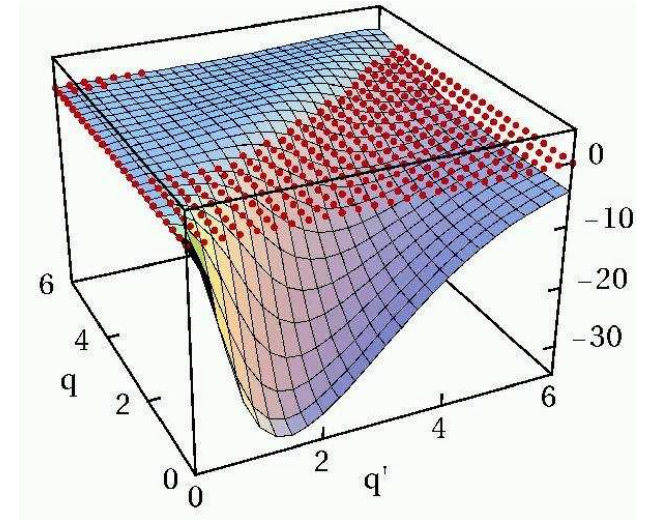
- Unitary Correlation Operator Method
- **Correlated Interaction in Momentum Space**

3S_1 bare



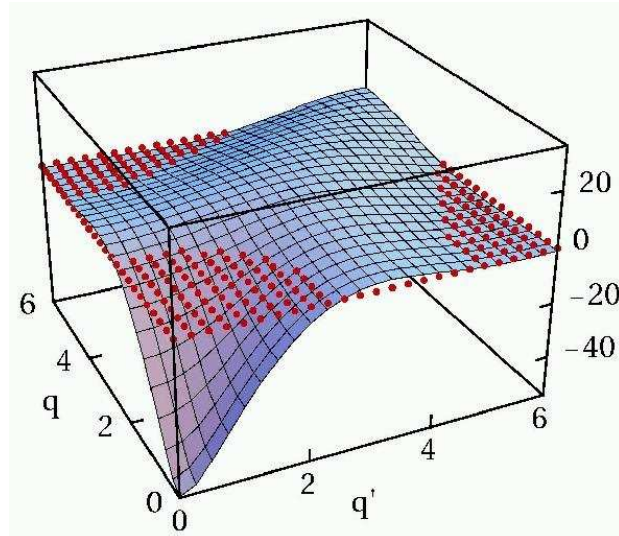
bare interaction has **strong off-diagonal** matrix elements connecting to high momenta

${}^3S_1 - {}^3D_1$ bare



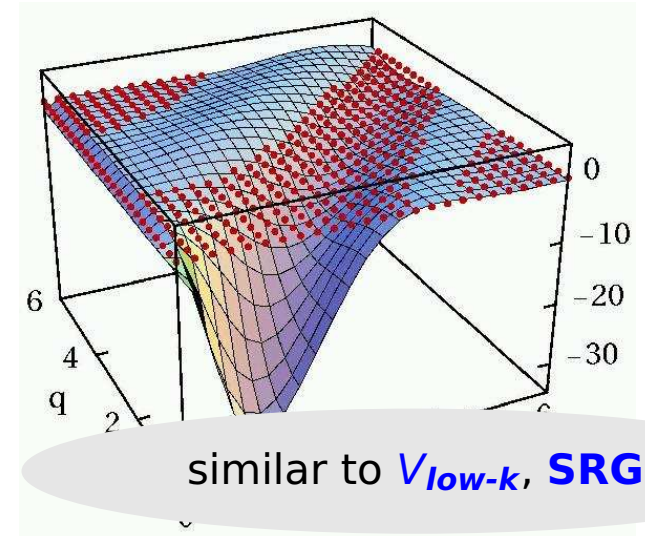
correlated interaction is **more attractive** at low momenta

3S_1 correlated



off-diagonal matrix elements connecting low- and high- momentum states are **strongly reduced**

${}^3S_1 - {}^3D_1$ correlated



similar to V_{low-k} , **SRG**

Fermionic Molecular Dynamics



Motivation

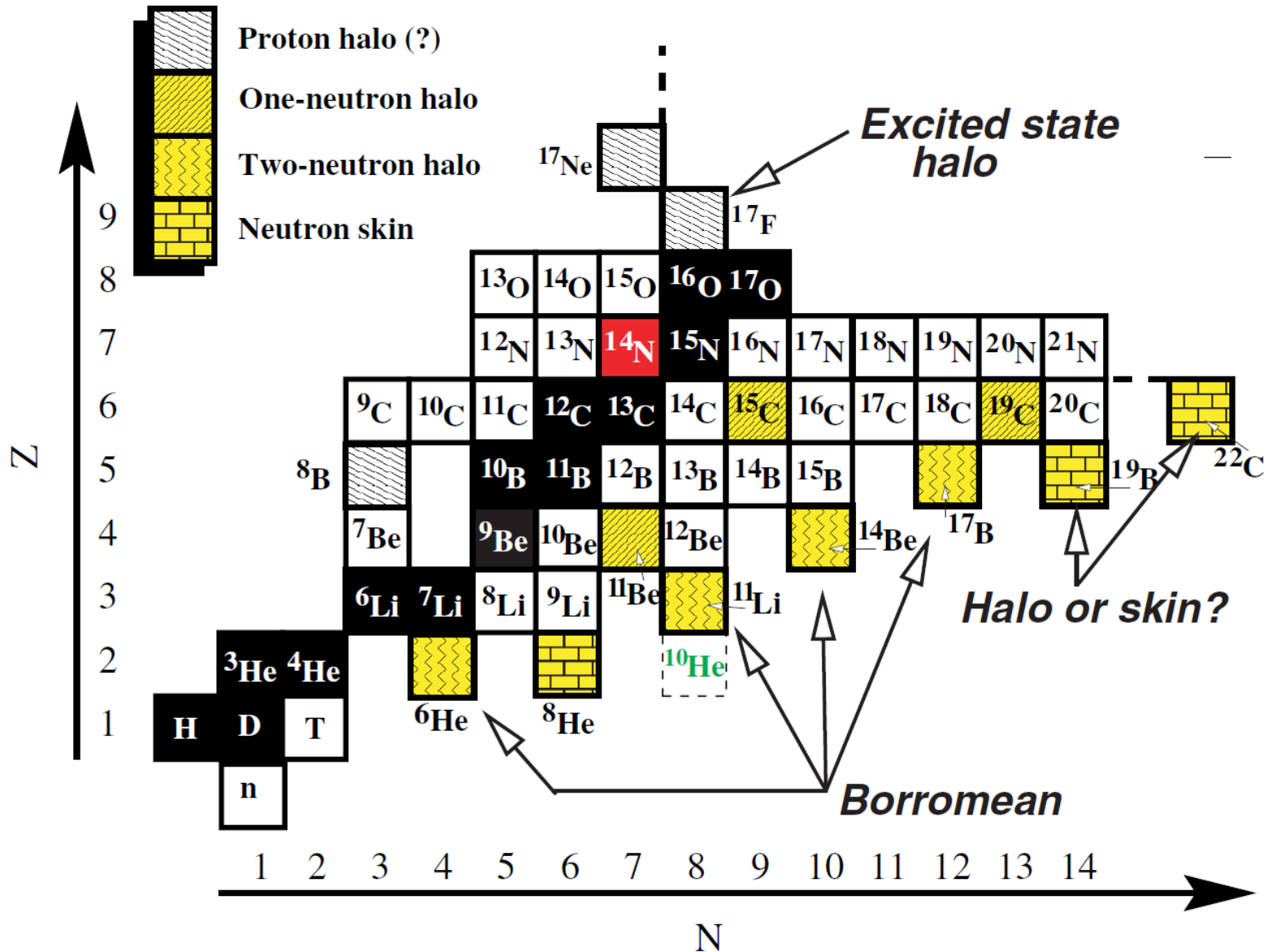
FMD Wave Functions

Nucleon-Nucleon Interaction

Mean-Field Calculations

**Projection After Variation,
Variation After Projection
and Multiconfiguration**

Exotica: Special Challenges



Fermionic

Slater determinant

$$|Q\rangle = \mathcal{A}\left(|q_1\rangle \otimes \cdots \otimes |q_A\rangle\right)$$

- antisymmetrized A -body state

Fermionic

Slater determinant

$$|Q\rangle = \mathcal{A}\left(|q_1\rangle \otimes \cdots \otimes |q_A\rangle\right)$$

- antisymmetrized A -body state

Molecular

single-particle states

$$\langle \mathbf{x} | q \rangle = \sum_i c_i \exp\left\{-\frac{(\mathbf{x} - \mathbf{b}_i)^2}{2a_i}\right\} \otimes |\chi_i^\uparrow, \chi_i^\downarrow\rangle \otimes |\xi\rangle$$

- Gaussian wave-packets in phase-space (complex parameter \mathbf{b}_i encodes mean position and mean momentum), spin is free, isospin is fixed
- width a_i is an independent variational parameter for each wave packet
- use one or two wave packets for each single particle state

Fermionic

Slater determinant

$$|Q\rangle = \mathcal{A}\left(|q_1\rangle \otimes \cdots \otimes |q_A\rangle\right)$$

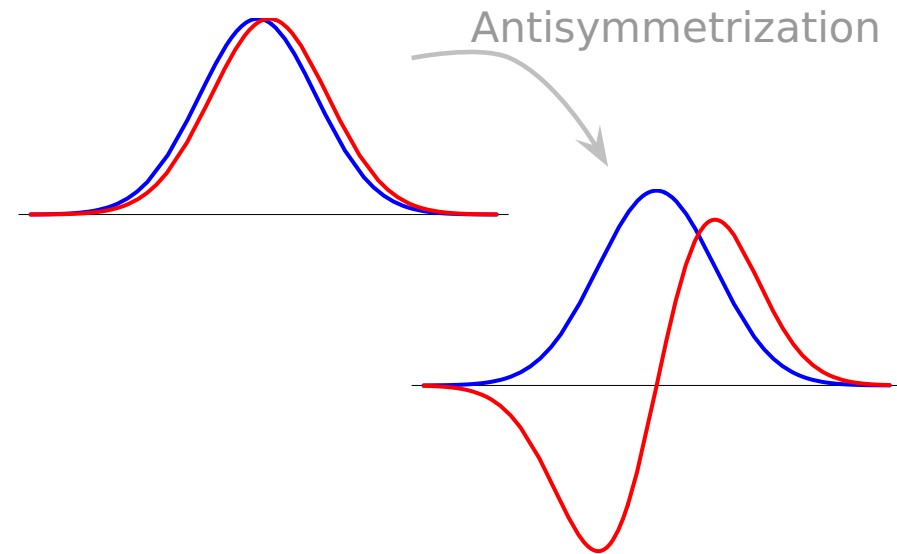
- antisymmetrized A -body state

Molecular

single-particle states

$$\langle \mathbf{x} | q \rangle = \sum_i c_i \exp\left\{-\frac{(\mathbf{x} - \mathbf{b}_i)^2}{2a_i}\right\} \otimes |\chi_i^\uparrow, \chi_i^\downarrow\rangle \otimes |\xi\rangle$$

- Gaussian wave-packets in phase-space (complex parameter \mathbf{b}_i encodes mean position and mean momentum), spin is free, isospin is fixed
- width a_i is an independent variational parameter for each wave packet
- use one or two wave packets for each single particle state



Fermionic Molecular Dynamics

Fermionic

Slater determinant

$$|Q\rangle = \mathcal{A}\left(|q_1\rangle \otimes \cdots \otimes |q_A\rangle\right)$$

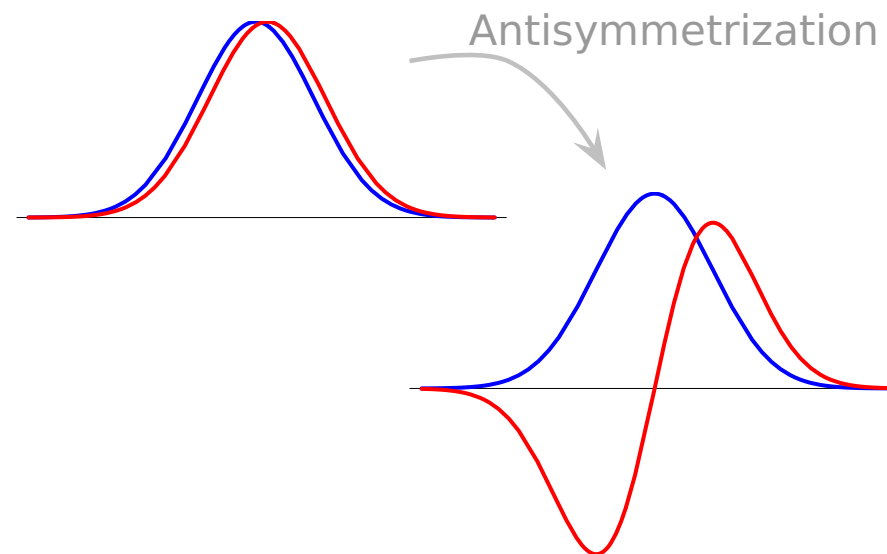
- antisymmetrized A-body state

Molecular

single-particle states

$$\langle \mathbf{x} | q \rangle = \sum_i c_i \exp\left\{-\frac{(\mathbf{x} - \mathbf{b}_i)^2}{2a_i}\right\} \otimes |\chi_i^\uparrow, \chi_i^\downarrow\rangle \otimes |\xi\rangle$$

- Gaussian wave-packets in phase-space (complex parameter \mathbf{b}_i encodes mean position and mean momentum), spin is free, isospin is fixed
- width a_i is an independent variational parameter for each wave packet
- use one or two wave packets for each single particle state



see also
**Antisymmetrized
 Molecular Dynamics**
 Horiuchi, Kanada-En'yo,
 Kimura, ...

Evaluation of Matrix Elements

➔ non-orthogonal basis, use inverse overlap matrix

One-Body Operators

$$\frac{\langle Q | \tilde{T}^{[1]} | Q \rangle}{\langle Q | Q \rangle} = \sum_{k,l}^A \langle q_k | \tilde{T}^{[1]} | q_l \rangle o_{lk}$$

Two-Body Operators

$$\frac{\langle Q | \tilde{V}^{[2]} | Q \rangle}{\langle Q | Q \rangle} = \frac{1}{2} \sum_{k,l,m,n}^A \langle q_k, q_l | \tilde{V}^{[2]} | q_m, q_n \rangle (o_{mk} o_{nl} - o_{ml} o_{nk})$$

$$o = n^{-1} = \left(\langle q_i | q_j \rangle \right)^{-1}$$

Interaction Matrix Elements

(One-body) Kinetic Energy

$$\langle q_k | \tilde{T} | q_l \rangle = \langle a_k \mathbf{b}_k | \tilde{T} | a_l \mathbf{b}_l \rangle \langle \chi_k | \chi_l \rangle \langle \xi_k | \xi_l \rangle$$

$$\langle a_k \mathbf{b}_k | \tilde{T} | a_l \mathbf{b}_l \rangle = \frac{1}{2m} \left(\frac{3}{a_k^* + a_l} - \frac{(\mathbf{b}_k^* - \mathbf{b}_l)^2}{(a_k^* + a_l)^2} \right) R_{kl}$$

(Two-body) Potential

→ fit radial dependencies by (a sum of) Gaussians

$$G(\mathbf{x}_1 - \mathbf{x}_2) = \exp \left\{ -\frac{(\mathbf{x}_1 - \mathbf{x}_2)^2}{2K} \right\}$$

→ Gaussian integrals

$$\langle a_k \mathbf{b}_k, a_l \mathbf{b}_l | \tilde{G} | a_m \mathbf{b}_m, a_n \mathbf{b}_n \rangle = R_{km} R_{ln} \left(\frac{K}{\alpha_{klmn} + K} \right)^{3/2} \exp \left\{ -\frac{\rho_{klmn}^2}{2(\alpha_{klmn} + K)} \right\}$$

→ analytical formulas for matrix elements

$$\alpha_{klmn} = \frac{a_k^* a_m}{a_k^* + a_m} + \frac{a_l^* a_n}{a_l^* + a_n}$$

$$\rho_{klmn} = \frac{a_m \mathbf{b}_k^* + a_k^* \mathbf{b}_m}{a_k^* + a_m} - \frac{a_n \mathbf{b}_l^* + a_l^* \mathbf{b}_n}{a_l^* + a_n}$$

$$R_{km} = \langle a_k \mathbf{b}_k | a_m \mathbf{b}_m \rangle$$

Operator Representation of V_{UCOM}

$$\tilde{\zeta}^\dagger (\tilde{T} + \tilde{V}) \tilde{\zeta} = \tilde{T}$$

$$+ \sum_{ST} \hat{V}_c^{ST}(r) + \frac{1}{2} (p_r^2 \hat{V}_{p^2}^{ST}(r) + \hat{V}_{p^2}^{ST}(r) p_r^2) + \hat{V}_{l^2}^{ST}(r) \mathbf{l}^2$$

one-body kinetic energy

central potentials

$$+ \sum_T \hat{V}_{ls}^T(r) \mathbf{l} \cdot \mathbf{s} + \hat{V}_{l^2ls}^T(r) \mathbf{l}^2 \mathbf{l} \cdot \mathbf{s}$$

spin-orbit potentials

$$+ \sum_T \hat{V}_t^T(r) \mathcal{S}_{12}(\mathbf{r}, \mathbf{r}) + \hat{V}_{trp_\Omega}^T(r) p_r \mathcal{S}_{12}(\mathbf{r}, \mathbf{p}_\Omega) + \hat{V}_{tll}^T(r) \mathcal{S}_{12}(\mathbf{l}, \mathbf{l}) +$$

$$\hat{V}_{tp_\Omega p_\Omega}^T(r) \mathcal{S}_{12}(\mathbf{p}_\Omega, \mathbf{p}_\Omega) + \hat{V}_{l^2tp_\Omega p_\Omega}^T(r) \mathbf{l}^2 \mathcal{S}_{12}(\mathbf{p}_\Omega, \mathbf{p}_\Omega)$$

tensor potentials

bulk of tensor force mapped onto central part
of correlated interaction

tensor correlations also change the spin-orbit
part of the interaction

Effective two-body interaction

- FMD model space can't describe correlations induced by residual medium-long ranged tensor forces
- use **long ranged tensor correlator – “low cutoff”** to partly account for that
- no three-body forces, missing spin-orbit strength, radii tend to be too small
- add phenomenological two-body correction term with a **momentum-dependent** central and (isospin-dependent) **spin-orbit** part (about 15% contribution to potential)
- fit correction term to binding energies and radii of “closed-shell” nuclei (${}^4\text{He}$, ${}^{16}\text{O}$, ${}^{40}\text{Ca}$), (${}^{24}\text{O}$, ${}^{34}\text{Si}$, ${}^{48}\text{Ca}$)

Outlook

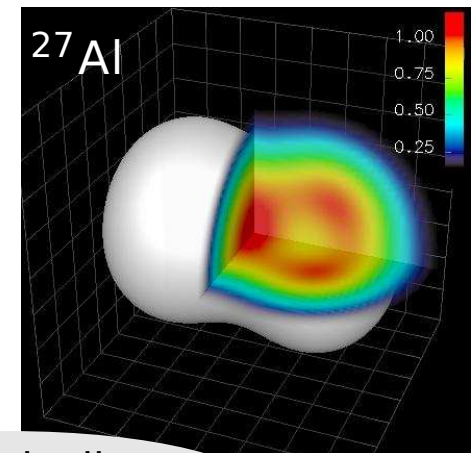
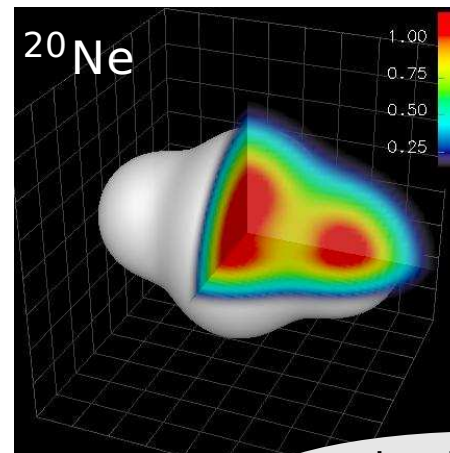
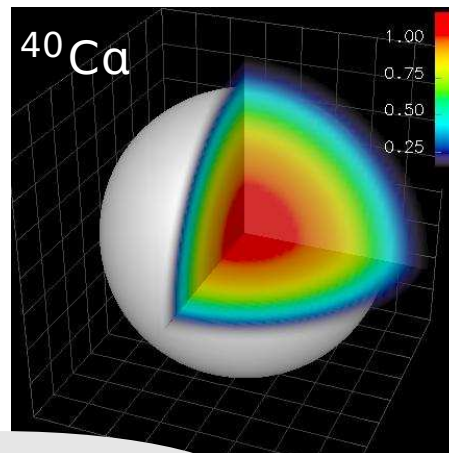
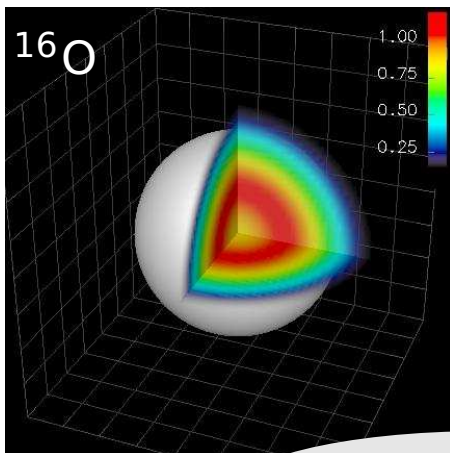
- use **UCOM(SRG)** and **SRG** interactions
- use **three-body** or **density dependent two-body force** instead of two-body correction term ?

Minimization

- minimize Hamiltonian expectation value with respect to all single-particle parameters q_k

$$\min_{\{q_k\}} \frac{\langle Q | \tilde{H} - \tilde{T}_{cm} | Q \rangle}{\langle Q | Q \rangle}$$

- this is a Hartree-Fock calculation in our particular single-particle basis
- the mean-field may break the symmetries of the Hamiltonian



spherical nuclei

intrinsically deformed nuclei

Projection After Variation (PAV)

- mean-field may break symmetries of Hamiltonian
- restore inversion, translational and rotational symmetry by projection on parity, linear and angular momentum

$$\tilde{P}^\pi = \frac{1}{2}(1 + \pi\Pi)$$

$$\tilde{P}_{MK}^J = \frac{2J+1}{8\pi^2} \int d^3\Omega D_{MK}^{J*}(\Omega) \tilde{R}(\Omega)$$

$$\tilde{P}^{\mathbf{P}} = \frac{1}{(2\pi)^3} \int d^3\mathbf{X} \exp\{-i(\tilde{\mathbf{P}} - \mathbf{P}) \cdot \mathbf{X}\}$$

Projection After Variation (PAV)

- mean-field may break symmetries of Hamiltonian
- restore inversion, translational and rotational symmetry by projection on parity, linear and angular momentum

$$\tilde{P}^\pi = \frac{1}{2}(1 + \pi\Pi)$$

$$\tilde{P}_{MK}^J = \frac{2J+1}{8\pi^2} \int d^3\Omega D_{MK}^{J*}(\Omega) \tilde{R}(\Omega)$$

Variation After Projection (VAP)

- effect of projection can be large
- full Variation after Angular Momentum and Parity Projection (VAP) for light nuclei
- perform VAP in GCM sense by applying **constraints** on **radius**, **dipole moment**, **quadrupole moment** or **octupole moment** and minimizing the energy in the projected energy surface for heavier nuclei

$$\tilde{P}^{\mathbf{P}} = \frac{1}{(2\pi)^3} \int d^3\mathbf{X} \exp\{-i(\tilde{\mathbf{P}} - \mathbf{P}) \cdot \mathbf{X}\}$$

PAV, VAP and Multiconfiguration

Projection After Variation (PAV)

- mean-field may break symmetries of Hamiltonian
- restore inversion, translational and rotational symmetry by projection on parity, linear and angular momentum

$$\tilde{P}^\pi = \frac{1}{2}(1 + \pi\Pi)$$

$$\tilde{P}_{MK}^J = \frac{2J+1}{8\pi^2} \int d^3\Omega D_{MK}^{J*}(\Omega) \tilde{P}(\Omega)$$

Variation After Projection (VAP)

- effect of projection can be large
- full Variation after Angular Momentum and Parity Projection (VAP) for light nuclei
- perform VAP in GCM sense by applying **constraints** on **radius**, **dipole moment**, **quadrupole moment** or **octupole moment** and minimizing the energy in the projected energy surface for heavier nuclei

$$\tilde{P}^{\mathbf{P}} = \frac{1}{(2\pi)^3} \int d^3\mathbf{X} \exp\{-i(\tilde{\mathbf{P}} - \mathbf{P}) \cdot \mathbf{X}\}$$

Multiconfiguration Calculations

- **diagonalize** Hamiltonian in a set of projected intrinsic states

$$\left\{ |Q^{(a)}\rangle, \quad a = 1, \dots, N \right\}$$

$$\sum_{K'b} \langle Q^{(a)} | \tilde{H} \tilde{P}_{KK'}^{J\pi} \tilde{P}^{\mathbf{P}=0} | Q^{(b)} \rangle \cdot c_{K'b}^\alpha = E^{J\pi\alpha} \sum_{K'b} \langle Q^{(a)} | \tilde{P}_{KK'}^{J\pi} \tilde{P}^{\mathbf{P}=0} | Q^{(b)} \rangle \cdot c_{K'b}^\alpha$$

Beryllium Isotopes



Questions

- α -clustering, halos in ^{11}Be and ^{14}Be , $N = 8$ shell closure ?

Calculation

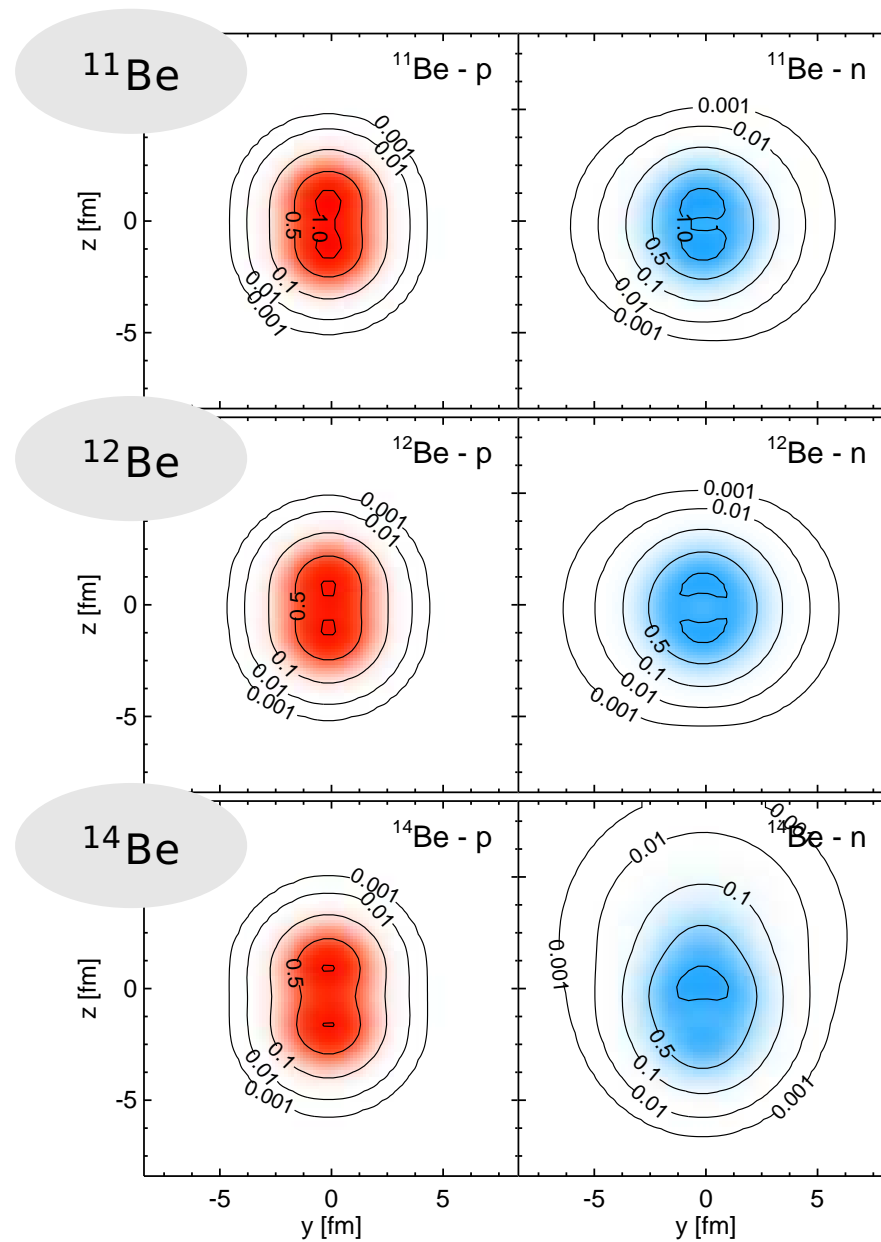
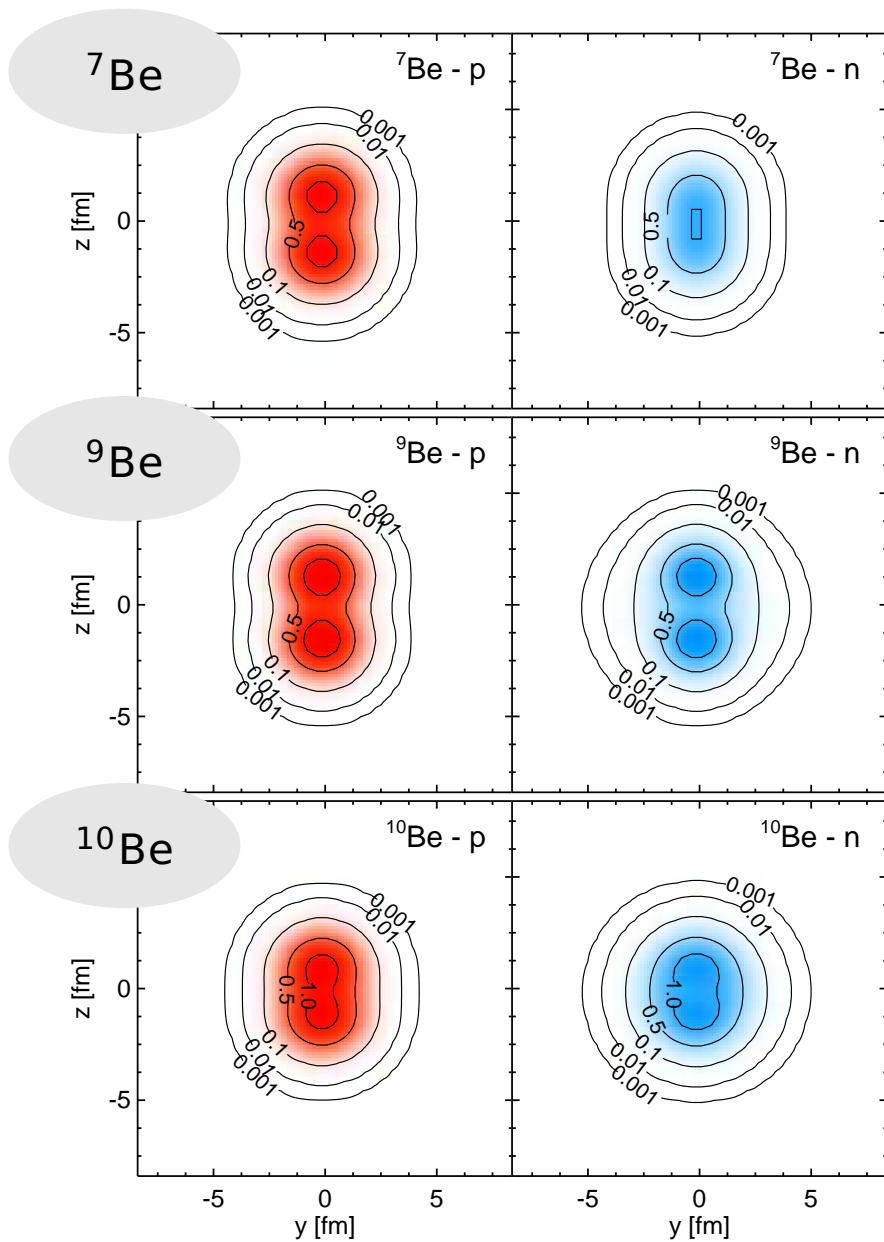
- FMD wave functions with two Gaussians per sp-state
- mean field, variation after projection, variation after multiconfiguration mixing
- VAP and multiconfiguration-VAP configurations with mean proton distance as generator coordinate

Observables

- energies
- charge and matter radii, electromagnetic transitions

Beryllium Isotopes

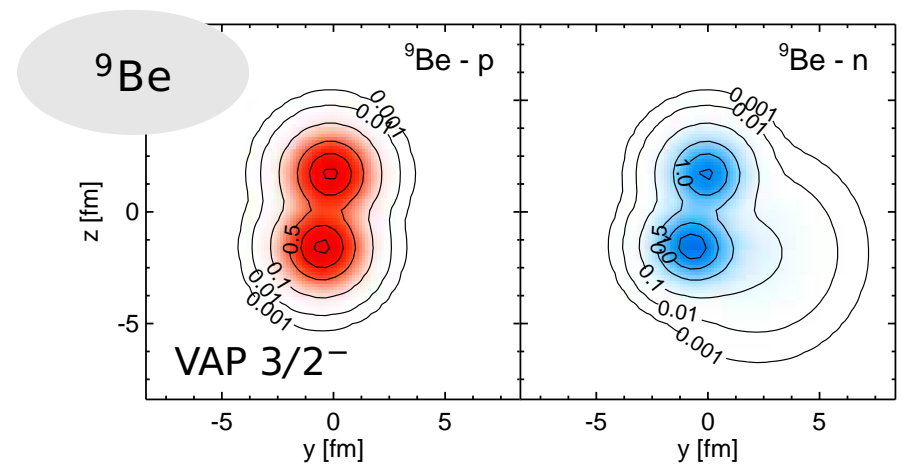
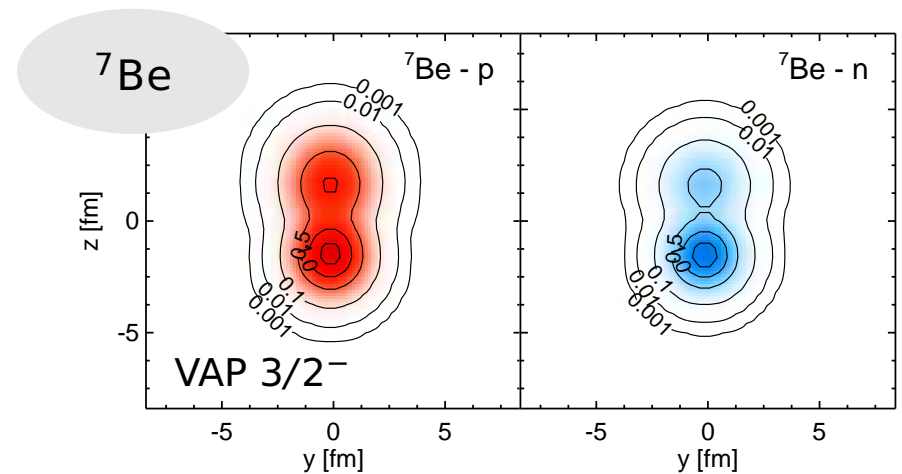
Mean field



Beryllium Isotopes

Variation after Projection

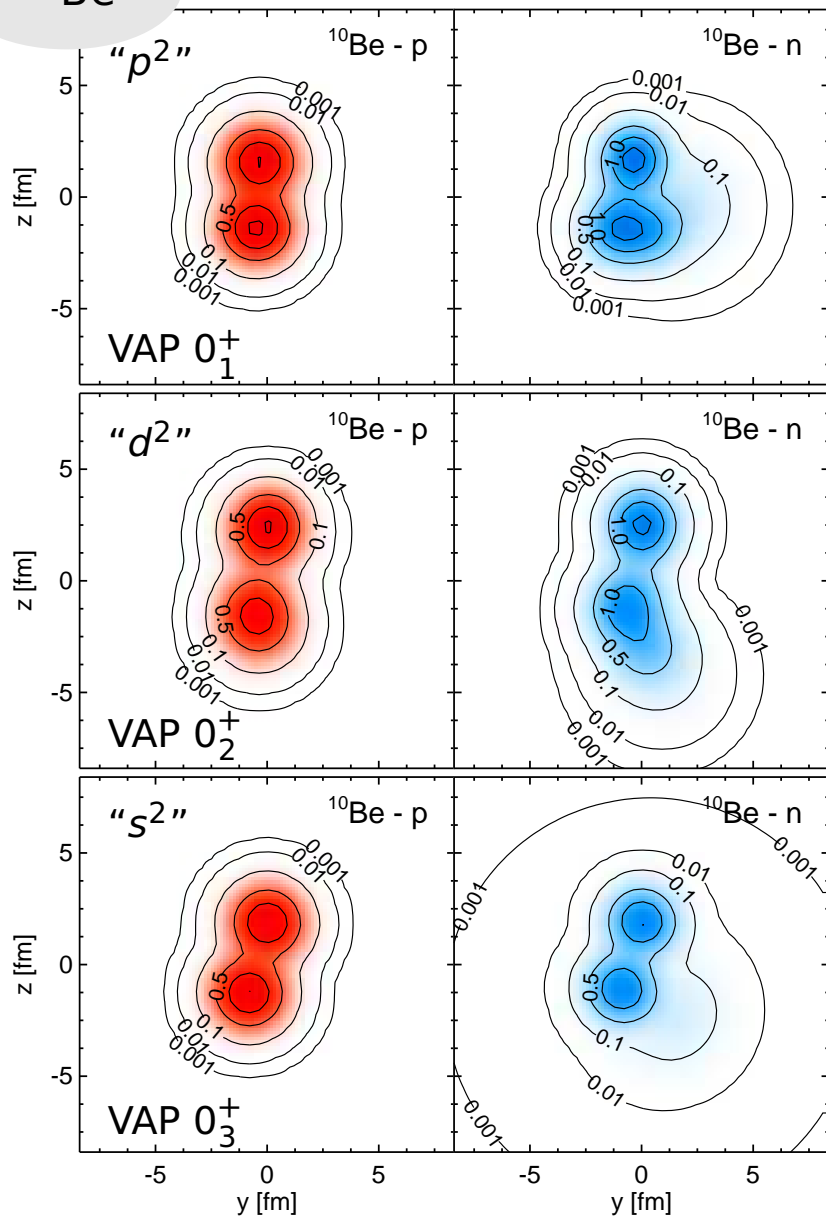
- create configurations by variation after parity and angular momentum projection
- large gain in binding energy compared to mean-field result
- intrinsic states show pronounced cluster structure. Parameters of ${}^4\text{He}$ and ${}^3\text{He}$ clusters are close to those of the free clusters



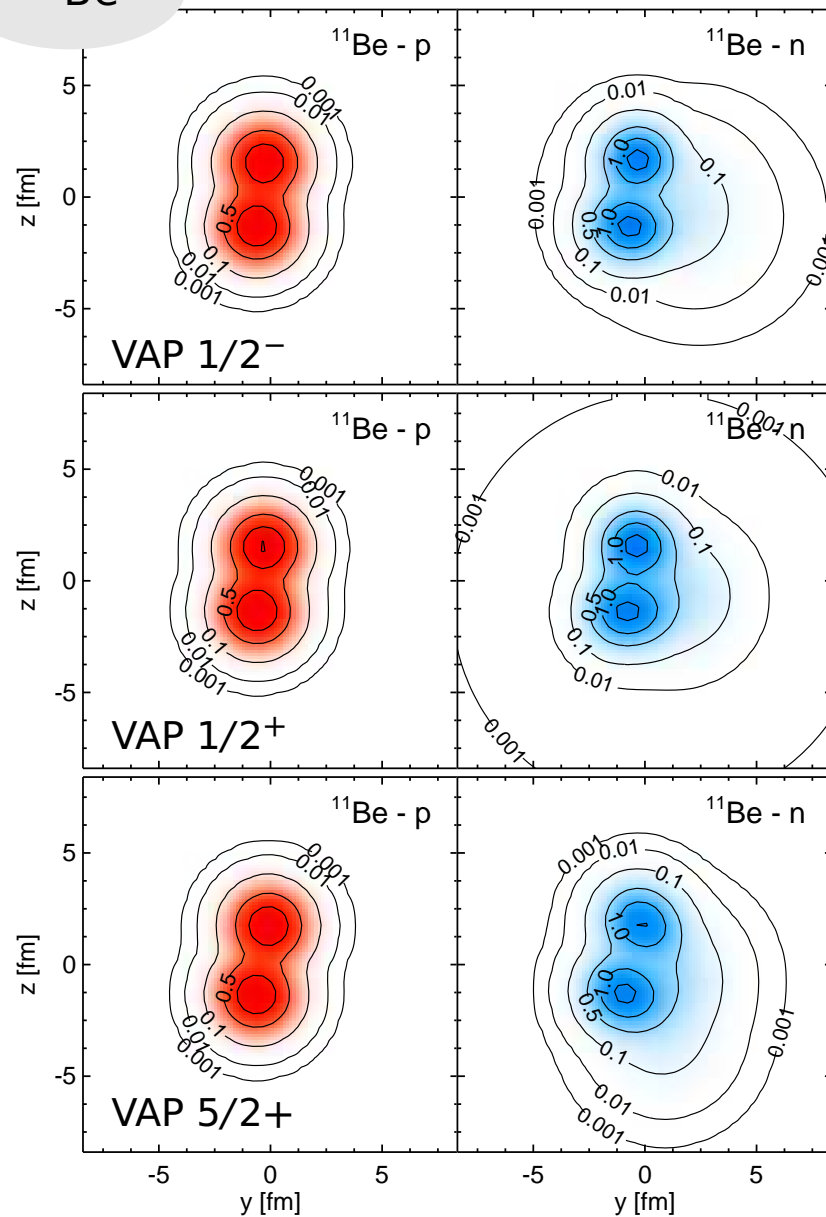
- Beryllium Isotopes

- Variation after Projection

^{10}Be



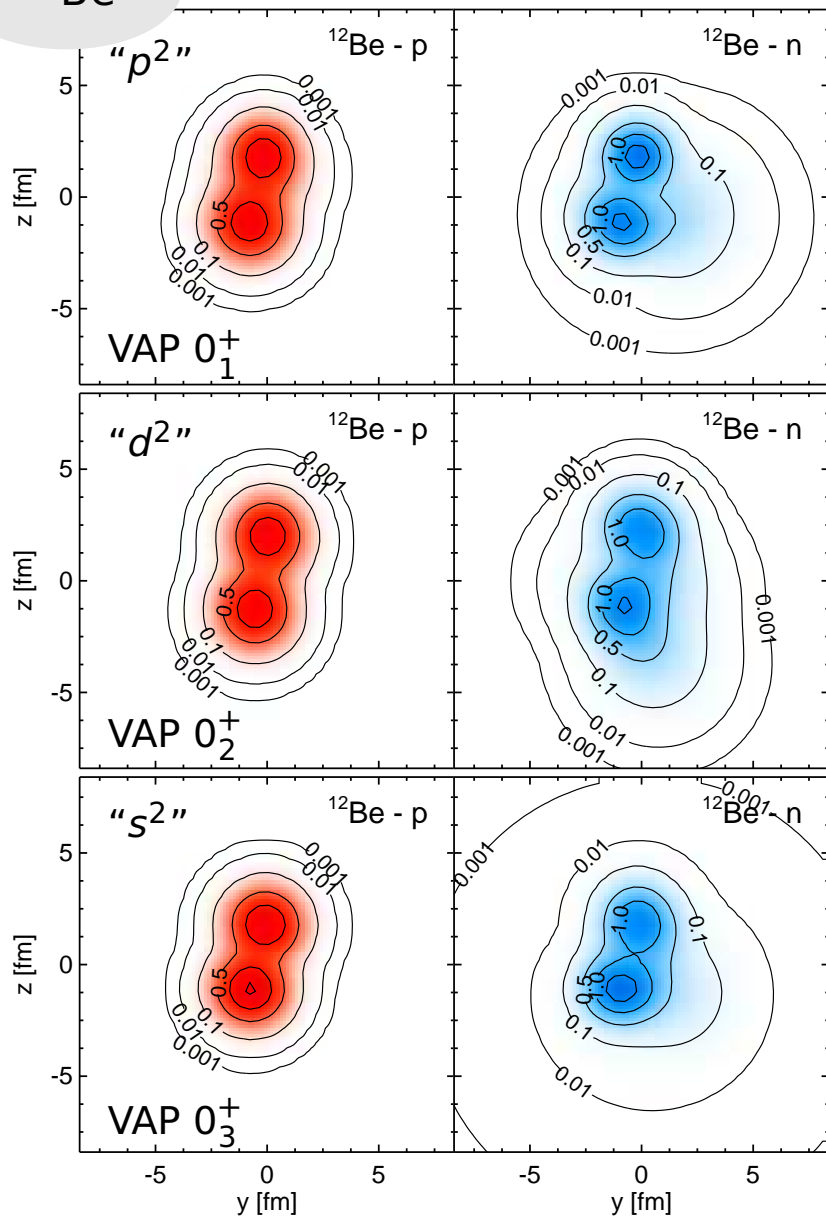
^{11}Be



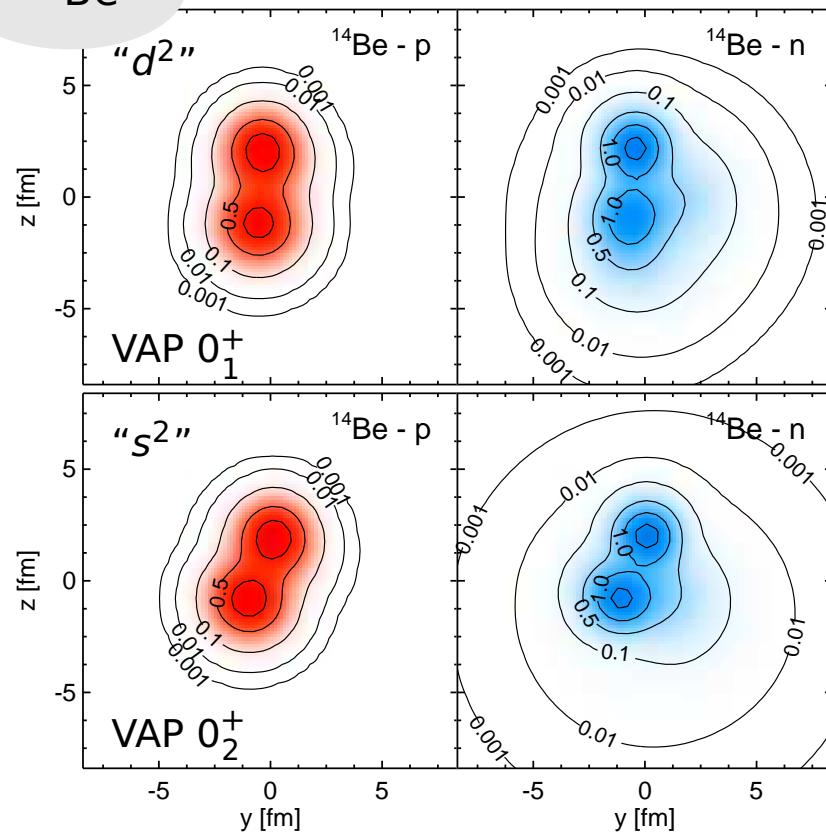
Beryllium Isotopes

Variation after Projection

^{12}Be

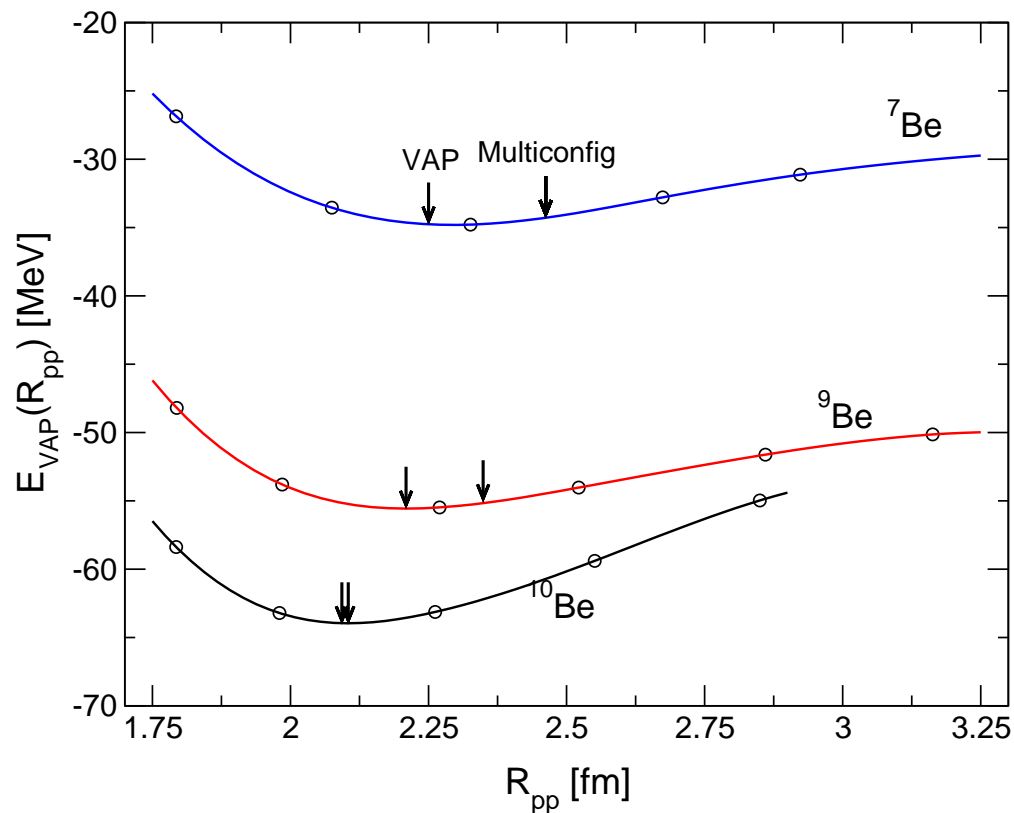


^{14}Be



- Beryllium Isotopes

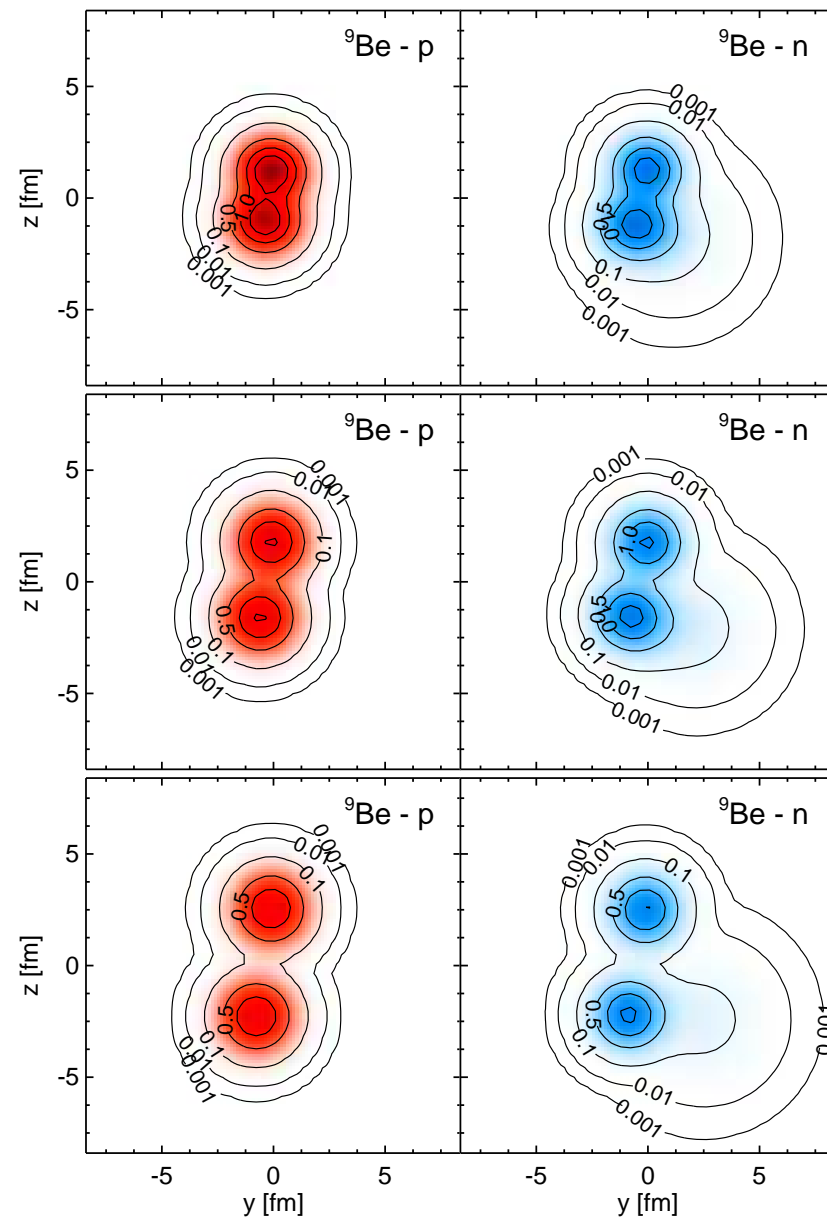
- Mean proton distance as generator coordinate



Mean proton distance

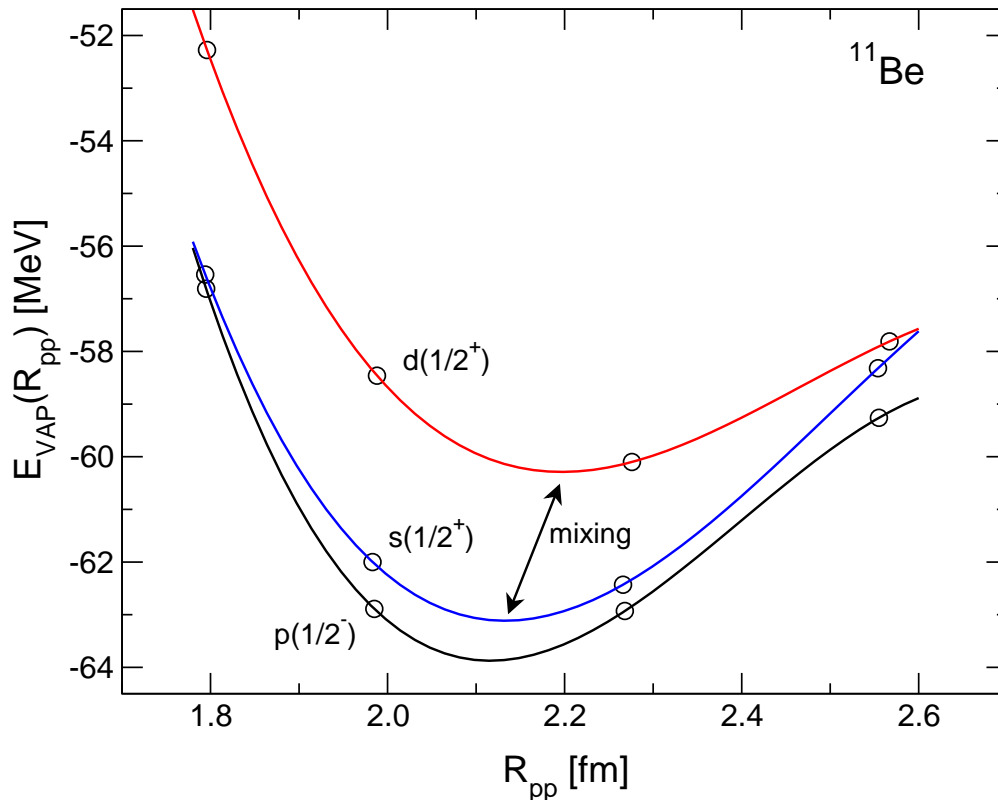
$$R_{pp}^2 = \frac{1}{Z^2} \left\langle \sum_{i < j}^{\text{protons}} (\mathbf{r}_i - \mathbf{r}_j)^2 \right\rangle$$

R_{pp} as a measure of α -cluster distance



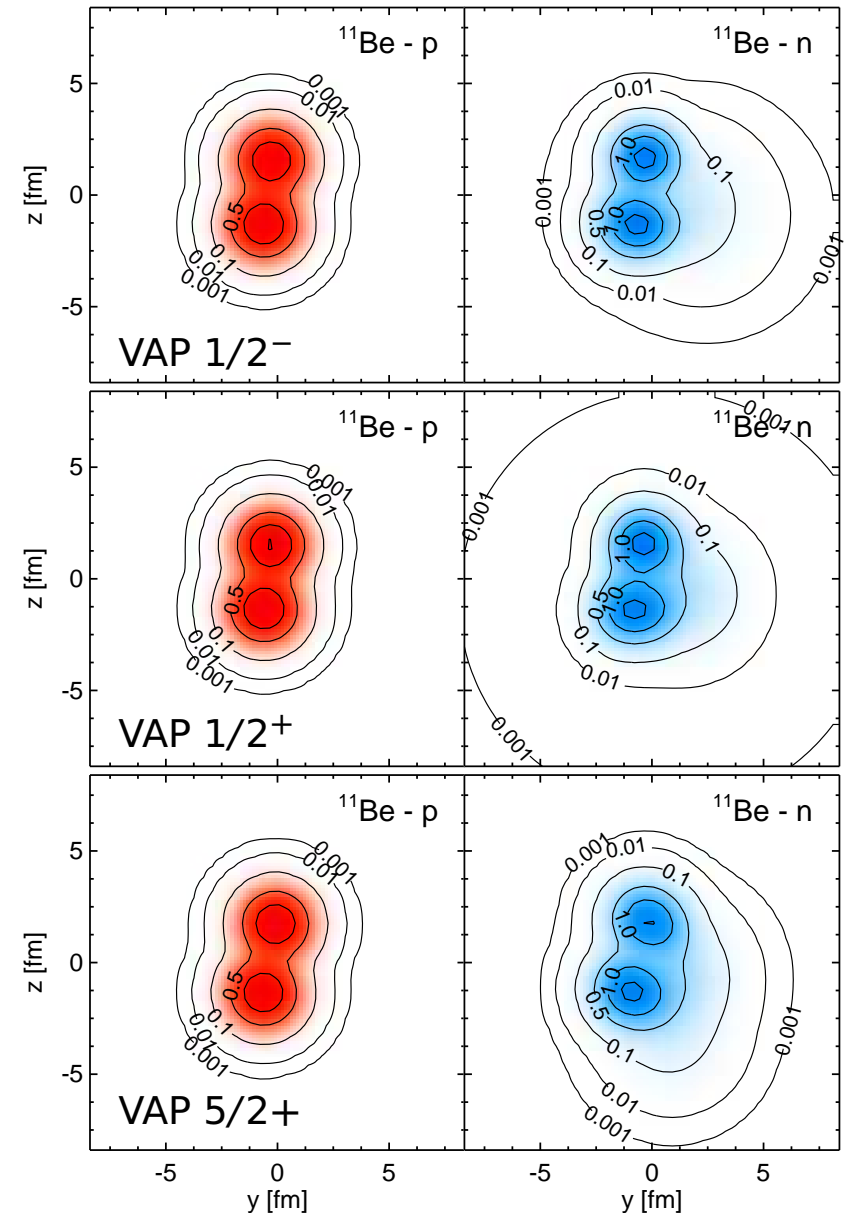
Beryllium Isotopes

Mean proton distance as generator coordinate



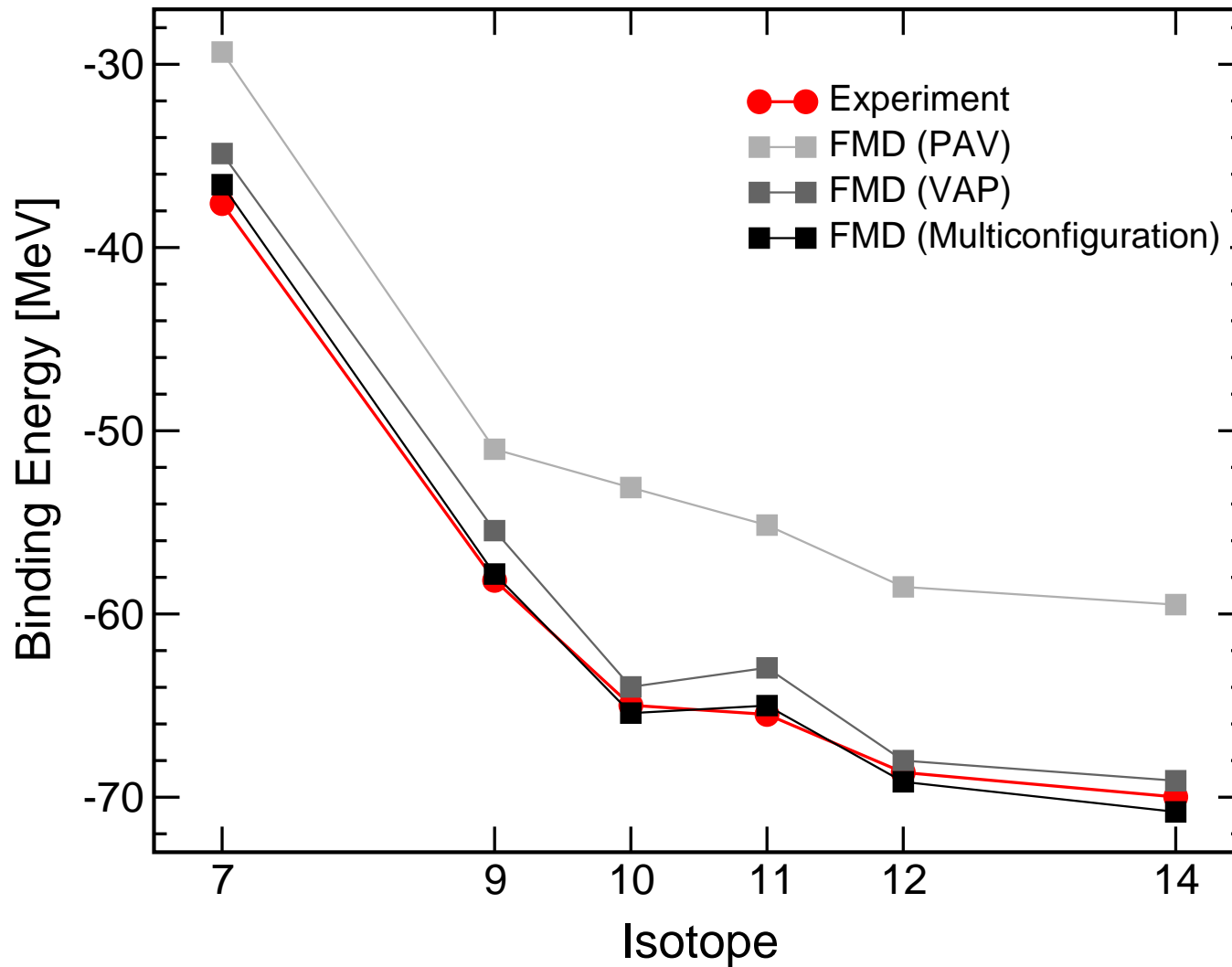
^{11}Be - "p", "s" and "d"-configurations

- "s"- and "d"-configurations will mix in $1/2^+$ state
- energy surfaces for "p" and "s" similar to those in ^{10}Be
- "d" surface has minimum at larger cluster distance \rightarrow d-configuration has a polarized ^{10}Be core



Beryllium Isotopes

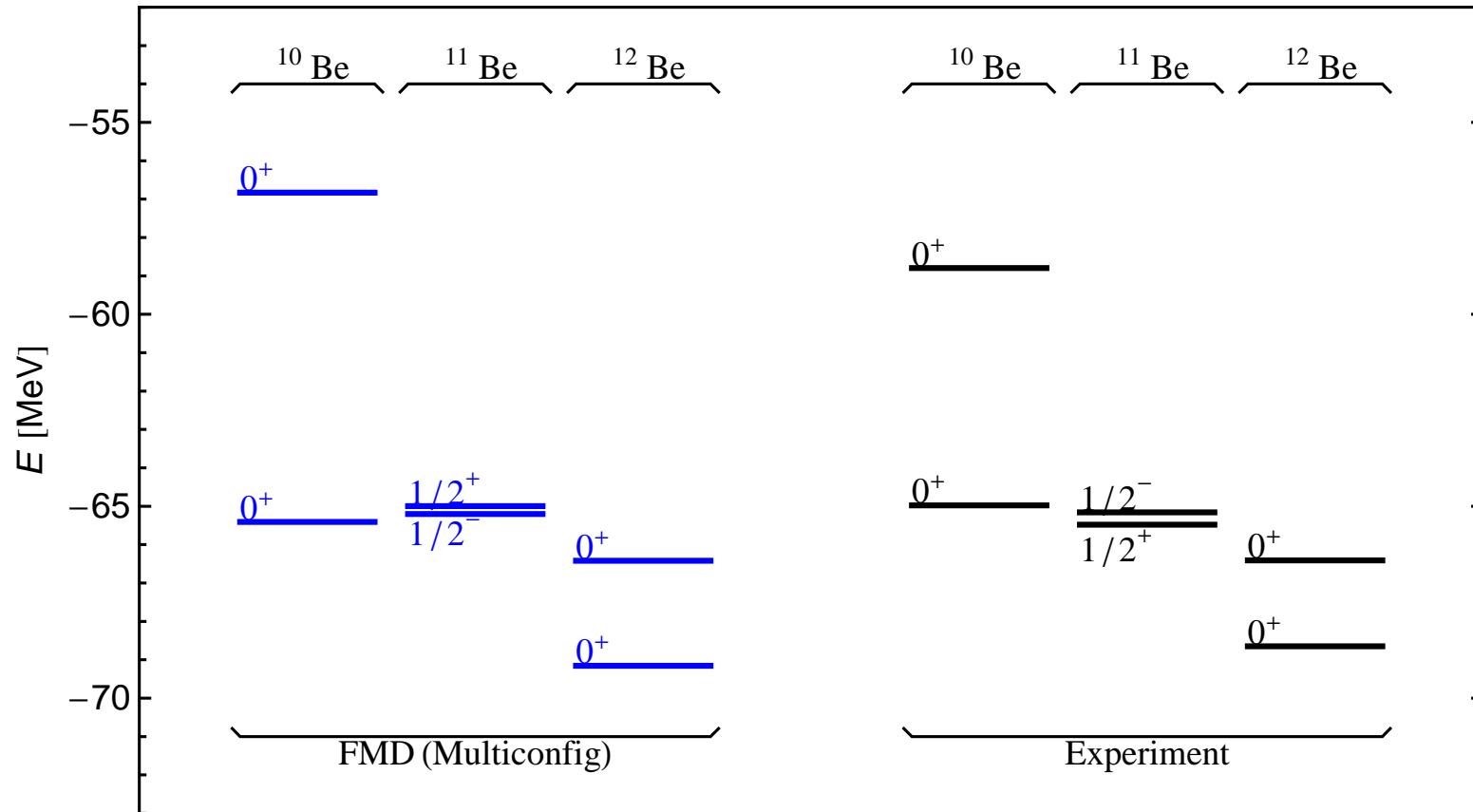
Binding energies



- large correlation energies due to cluster structure
- loosely bound systems gain most by configuration mixing

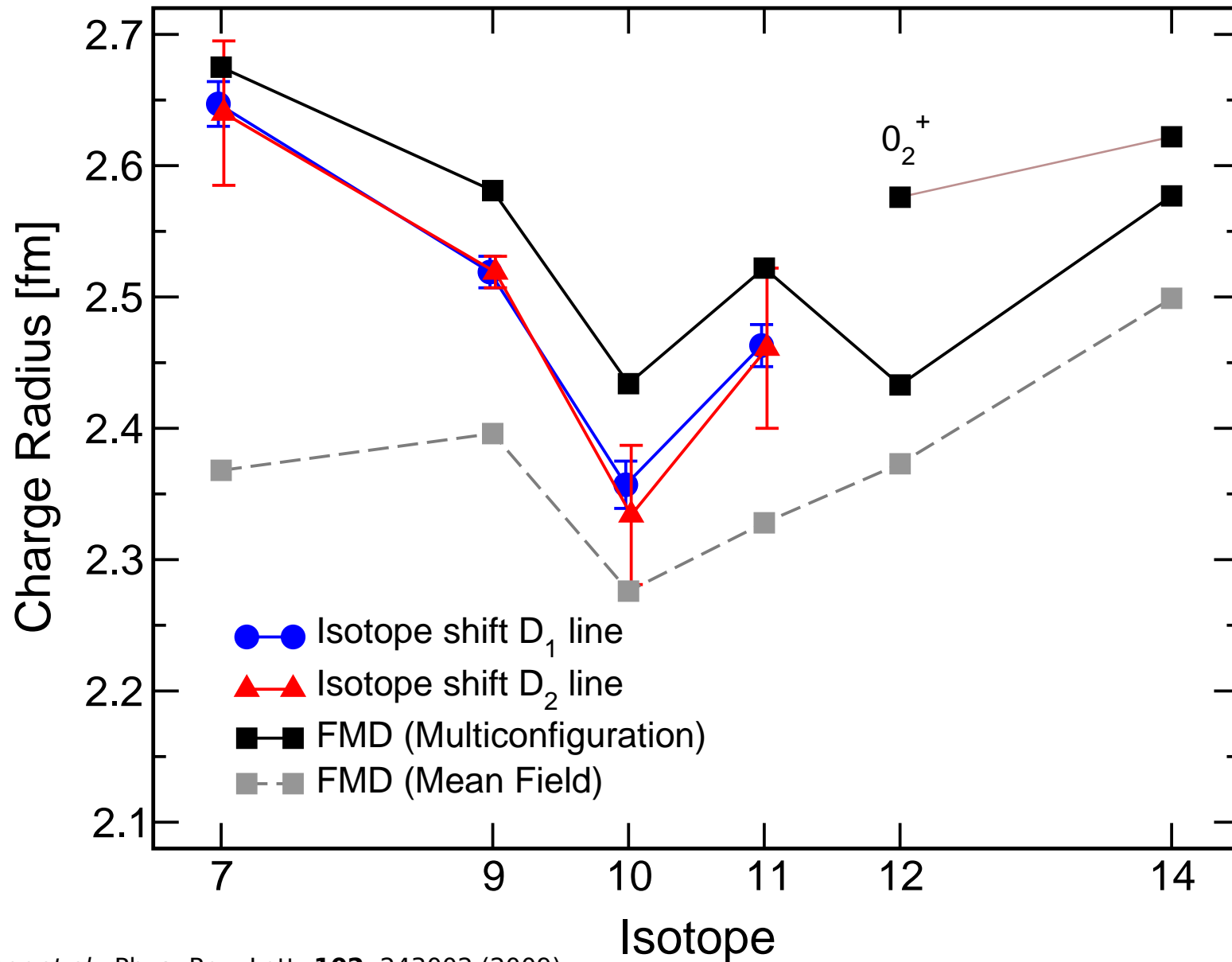
Beryllium Isotopes

$N = 8$ Shell Closure ?



- "almost correct" level ordering in ^{11}Be
- ^{12}Be ground state dominated by p^2 configuration, sizeable admixture of s^2 and d^2 configurations which strongly mix

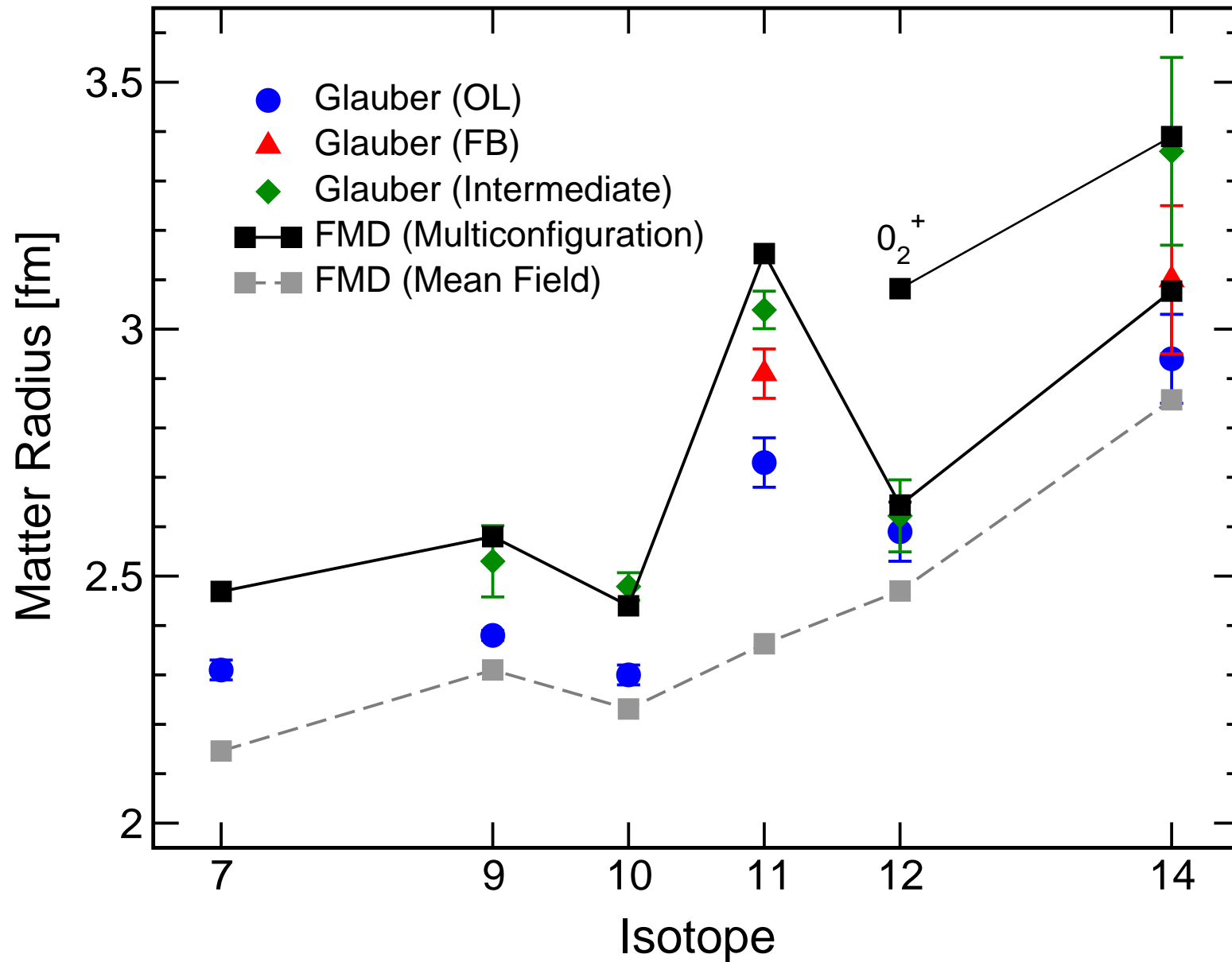
Beryllium Isotopes Charge Radii



Nörtershäuser *et al.*, Phys. Rev. Lett. **102**, 243002 (2009)

Zakova, Neff, *et al.*, J. Phys. G. **37**, 055107 (2010)

Beryllium Isotopes Matter Radii



Beryllium Isotopes

Electromagnetic transitions

^{10}Be

	FMD(Multiconfig)	Experiment
$B(E2; 2_1^+ \rightarrow 0_1^+)$	$11.27 e^2\text{fm}^4$	$9.2 \pm 0.3 e^2\text{fm}^4$
$B(E2; 2_2^+ \rightarrow 0_1^+)$	$1.00 e^2\text{fm}^4$	$0.11 \pm 0.02 e^2\text{fm}^4$
$B(E2; 0_2^+ \rightarrow 2_1^+)$	$4.99 e^2\text{fm}^4$	$3.2 \pm 1.9 e^2\text{fm}^4$
$B(E1; 0_2^+ \rightarrow 1_1^-)$	$0.013 e^2\text{fm}^2$	$0.013 \pm 0.004 e^2\text{fm}^2$

^{11}Be

	FMD(Multiconfig)	Experiment
$B(E1; 1/2_1^+ \rightarrow 1/2_1^-)$	$0.020 e^2\text{fm}^2$	$0.099 \pm 0.010 e^2\text{fm}^2$

^{12}Be

	FMD(Multiconfig)	Experiment
$B(E2; 2_1^+ \rightarrow 0_1^+)$	$8.27 e^2\text{fm}^4$	$8.0 \pm 3.0 e^2\text{fm}^4$
$B(E2; 0_2^+ \rightarrow 2_1^+)$	$6.50 e^2\text{fm}^4$	$7.0 \pm 0.6 e^2\text{fm}^4$
$M(E0; 0_1^+ \rightarrow 0_2^+)$	$1.05 e\text{fm}^2$	$0.87 \pm 0.03 e\text{fm}^2$
$B(E1; 0_1^+ \rightarrow 1_1^-)$	$0.08 e^2\text{fm}^2$	$0.051 \pm 0.003 e^2\text{fm}^2$

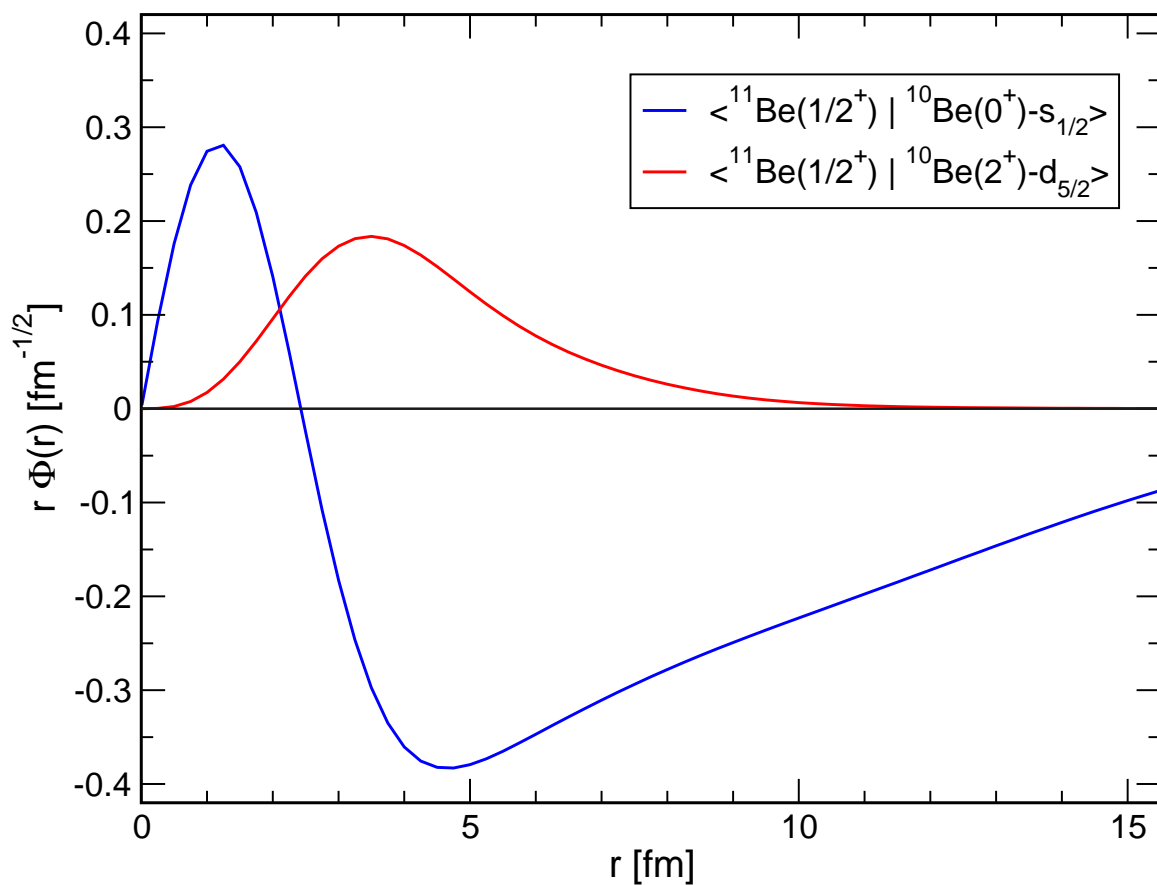
McCutchan *et al.*, Phys. Rev. Lett. **103**, 192501 (2009).

Nakamura *et al.*, Phys. Lett. **B394**, 11 (1997).

Shimoura *et al.*, Phys. Lett. **B654**, 87 (2007).

Iwasaki *et al.*, Phys. Lett. **B491**, 8 (2000).

^{11}Be - ^{10}Be Overlaps



Spectroscopic Factors

^{11}Be	^{10}Be	l_j	S
$1/2^+$	0^+	$s_{1/2}$	0.937
	2^+	$d_{5/2}$	0.094
	2^+	$d_{3/2}$	0.007
$5/2^+$	0^+	$d_{5/2}$	0.543
	2^+	$s_{1/2}$	0.329
	2^+	$d_{5/2}$	0.243
$1/2^-$	0^+	$p_{1/2}$	0.805
	2^+	$p_{3/2}$	0.779

- extended s-wave halo
- $s_{1/2}$ spectroscopic factor larger than results obtained from knockout and transfer reactions

Neon Isotopes ^{17}Ne - ^{22}Ne



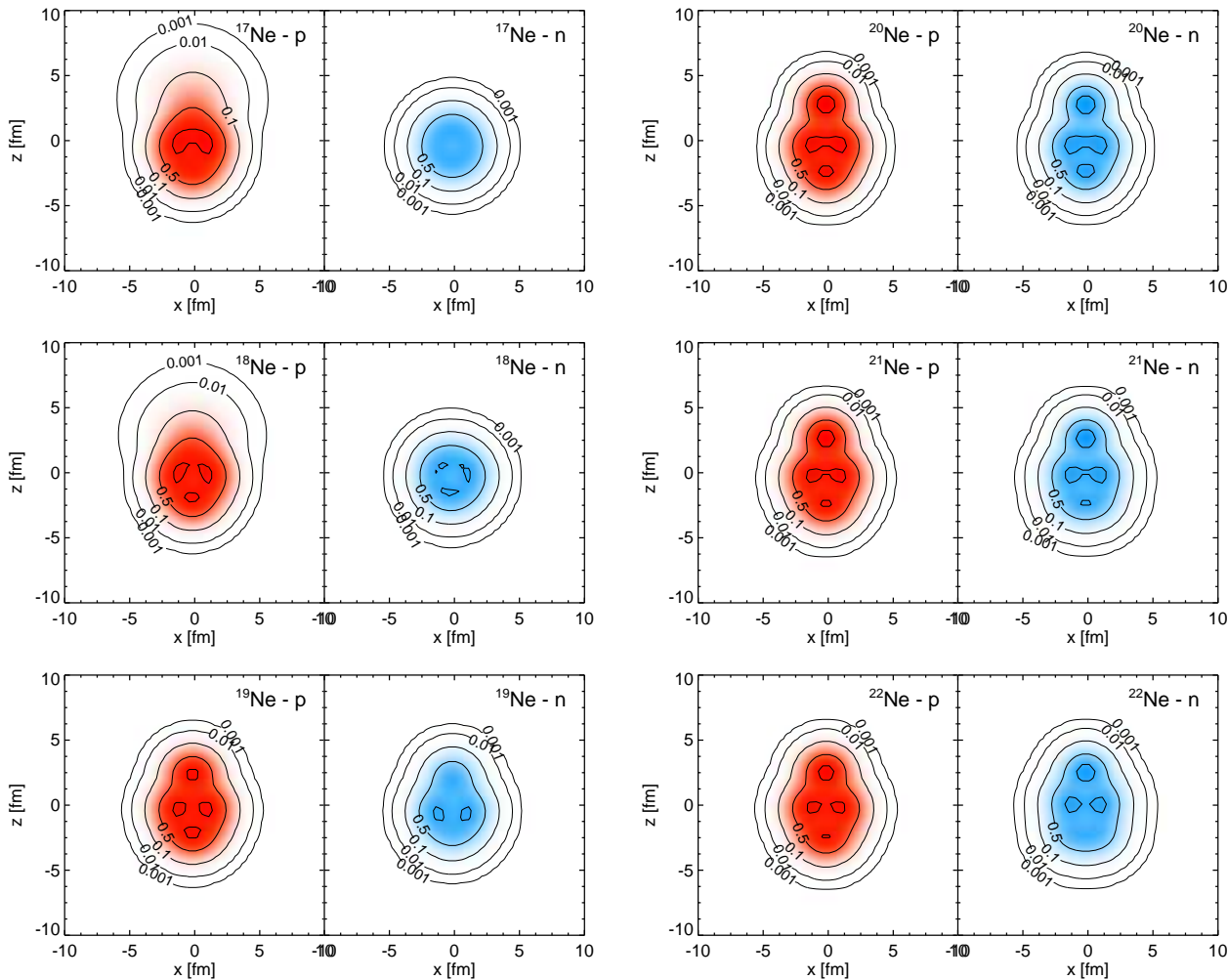
Structure

- s^2/d^2 occupation in ^{17}Ne and ^{18}Ne
- ^3He and ^4He cluster admixtures

Observables

- Charge Radii
- Matter Radii
- Electromagnetic transitions
- Rotational bands

Neon Isotopes Calculation



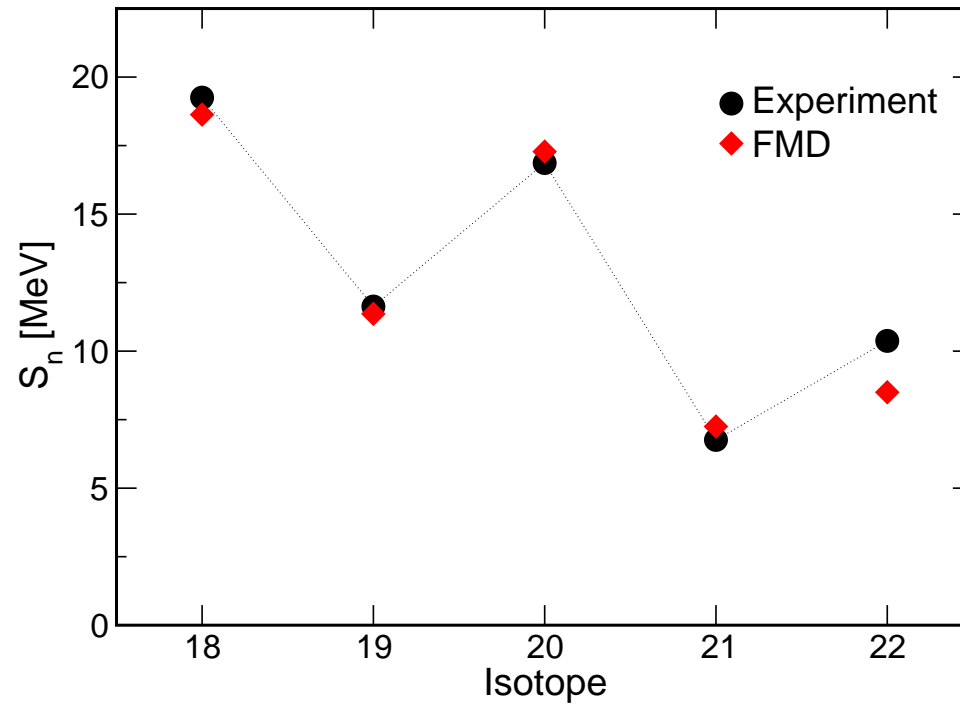
- Variation after parity projection on positive and negative parity
- Crank strength of spin-orbit force – changes properties of single-particle orbits and their occupations
- $^{15,16}\text{O}$ -“ s^2 ” and $^{15,16}\text{O}$ -“ d^2 ” minima in $^{17,18}\text{Ne}$
- explicit cluster configurations:
 - ^{17}Ne : ^{14}O - ^3He
 - ^{18}Ne : ^{14}O - ^4He
 - ^{19}Ne : ^{16}O - ^3He and ^{15}O - ^4He
 - ^{20}Ne : ^{16}O - ^4He
 - ^{21}Ne : “ ^{17}O ”- ^4He
 - ^{22}Ne : “ ^{18}O ”- ^4He

Intrinsic proton/neutron densities of dominant FMD configuration

Neon Isotopes

Separation energies

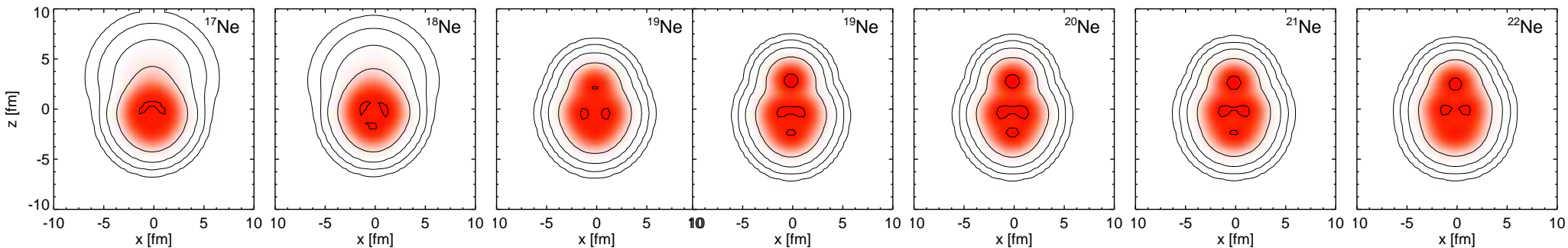
Separation Energies



17,18Ne: s^2/d^2 admixture

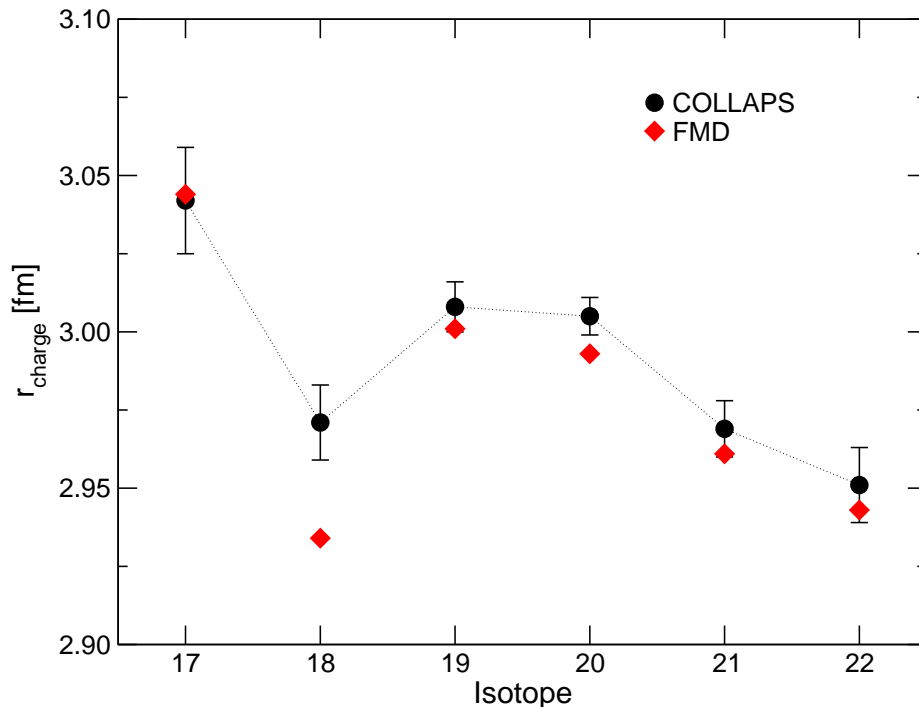
19Ne: ^3He , α clustering

20-22Ne: α clustering

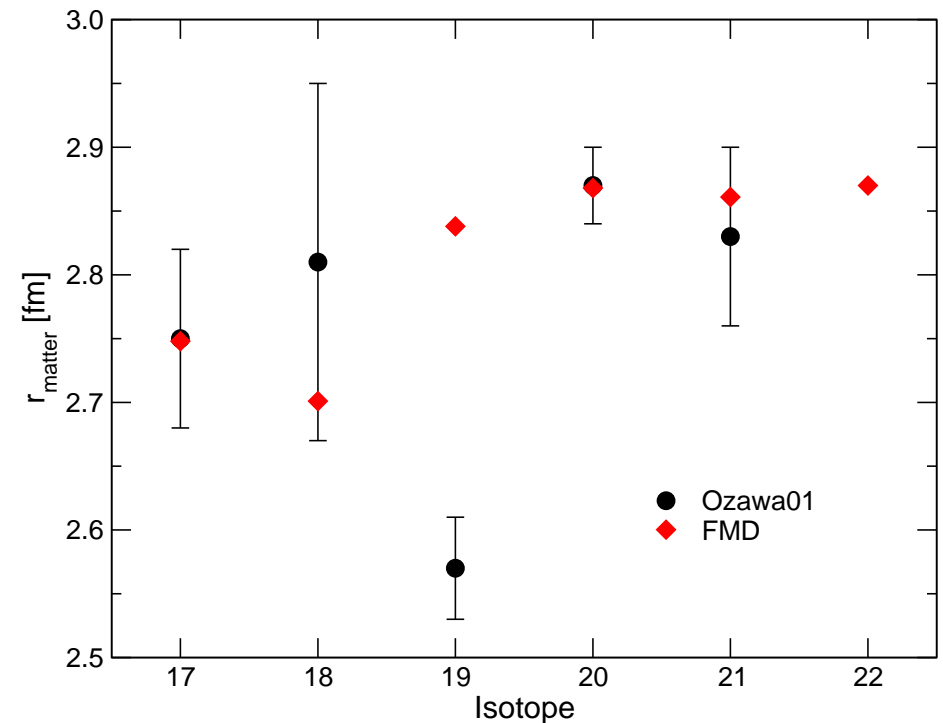


Neon Isotopes

Charge and Matter Radii



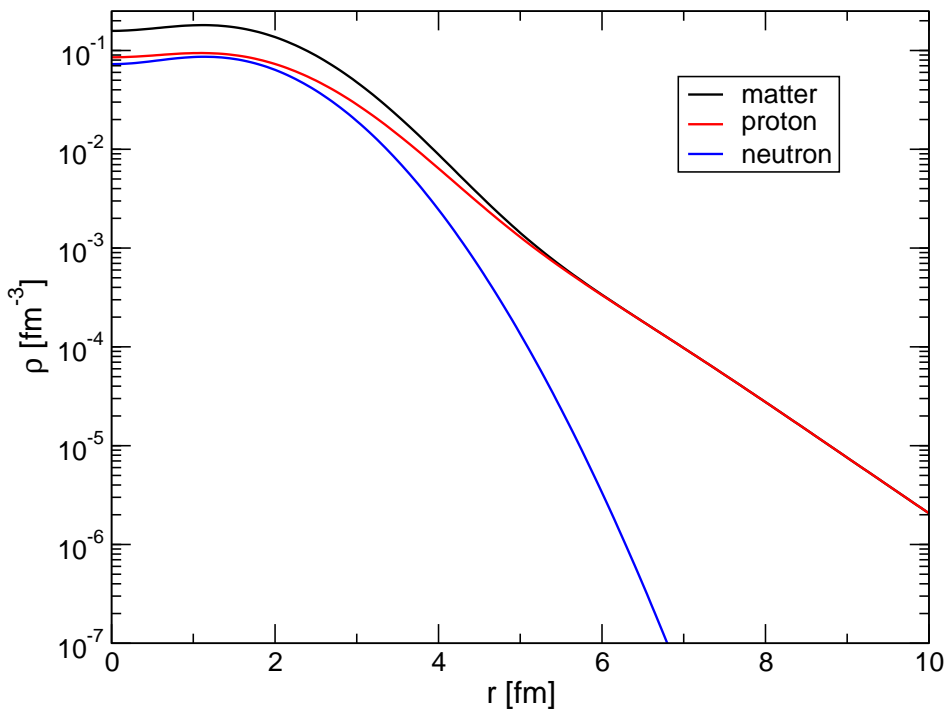
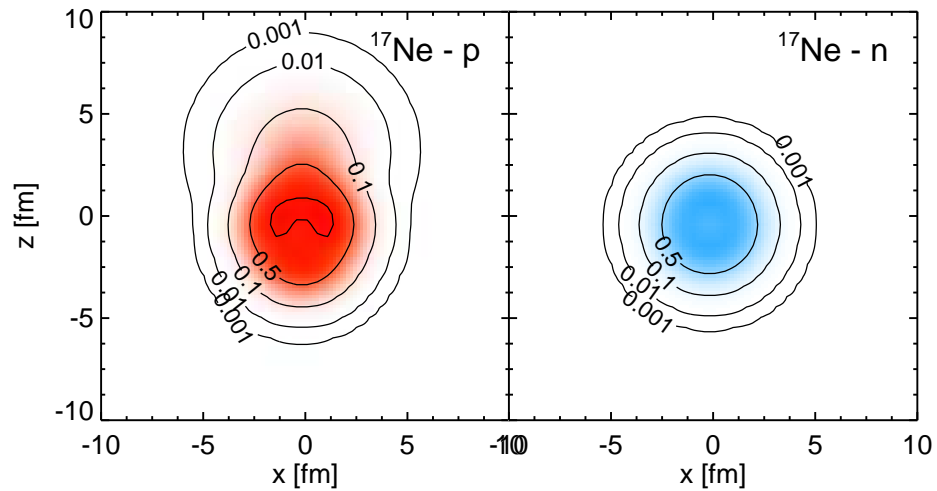
- charge radii of $^{17,18}\text{Ne}$ depend strongly on s^2/d^2 occupations
- cluster admixtures responsible for large charge radii in $^{19-22}\text{Ne}$
- measurements of charge radii by COLLAPS@ISOLDE, masses from ISOLTRAP@ISOLDE



- matter radii from interaction cross sections
A. Ozawa *et al.*, Nuc. Phys. **A693** (2001) 32
- good agreement with expectation of ^{19}Ne

Neon Isotopes

^{17}Ne Halo ?



	FMD	Experiment
$r_{\text{ch}}[\text{fm}]$	3.04	3.042(21)
$r_{\text{mat}}[\text{fm}]$	2.75	2.75(7) ¹
$B(E2; \frac{1}{2}^- \rightarrow \frac{3}{2}^-)[e^2\text{fm}^4]$	76.7	66^{+18}_{-25} ²
$B(E2; \frac{1}{2}^- \rightarrow \frac{5}{2}^-)[e^2\text{fm}^4]$	119.8	124(18) ²
occupancy s^2	42%	
occupancy d^2	55%	

- proton skin $r_p - r_n = 0.45$ fm
- 40% probability to find a proton at $r > 5$ fm

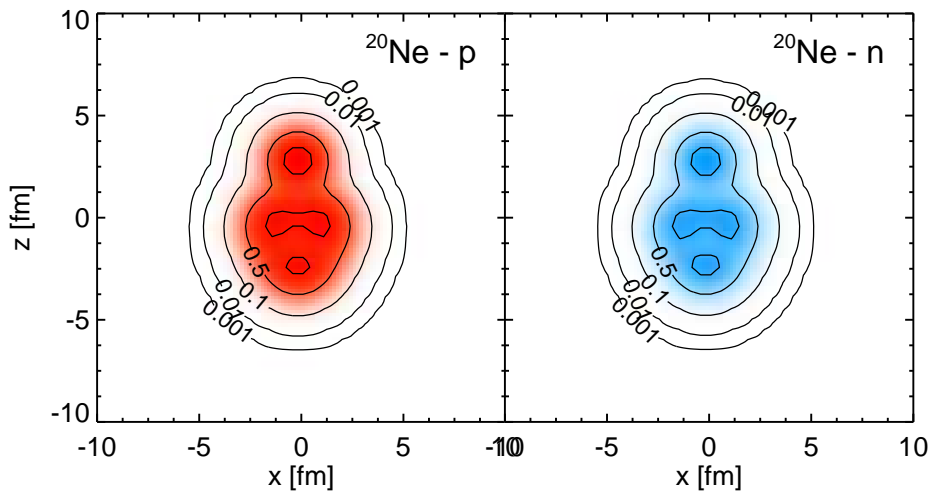
¹ A. Ozawa *et al.*, Nuc. Phys. **A693**, 32 (2001)

² M. J. Chromik *et al.*, Phys. Rev. C **66**, 024313 (2002)

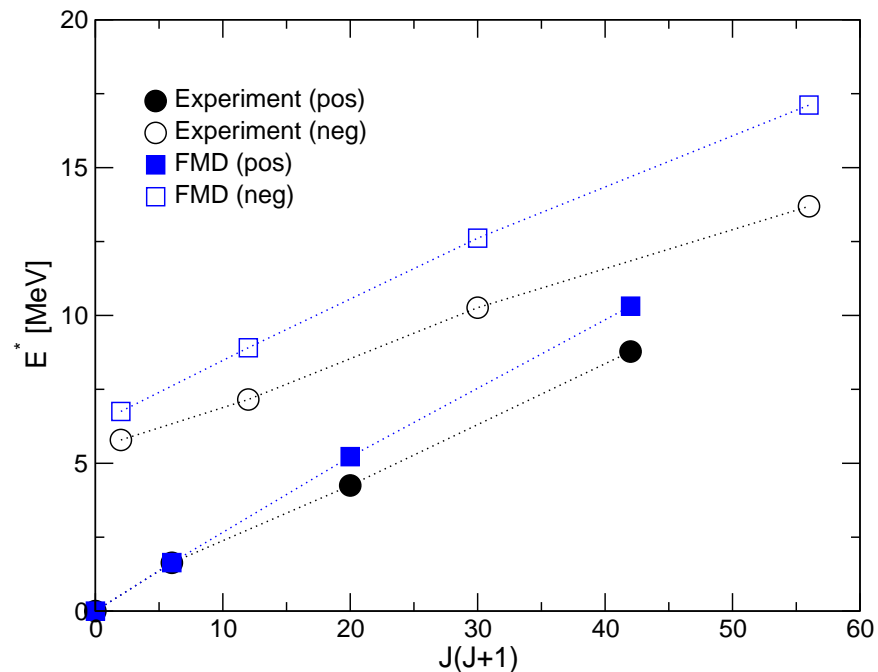
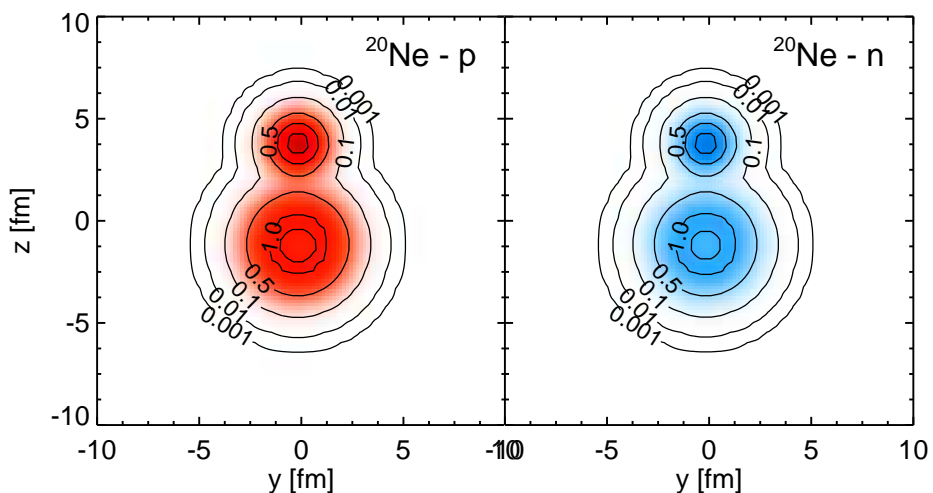
Neon Isotopes

^{20}Ne

positive parity



negative parity



	FMD	Experiment
r_{ch} [fm]	2.99	3.005(6)
r_{mat} [fm]	2.87	2.87(3)
$B(E2; 0^+ \rightarrow 2^+)$ [$e^2\text{fm}^4$]	275	340(30)
$S_{4\text{He}}(0^+)$	0.76	
$S_{4\text{He}}(1^-)$	0.97	

${}^3\text{He}(\alpha, \gamma){}^7\text{Be}$ radiative capture



Effective Nucleon-Nucleon interaction:

UCOM(SRG)

- $\lambda = 1.5\text{fm}^{-1}$, no phenomenological corrections

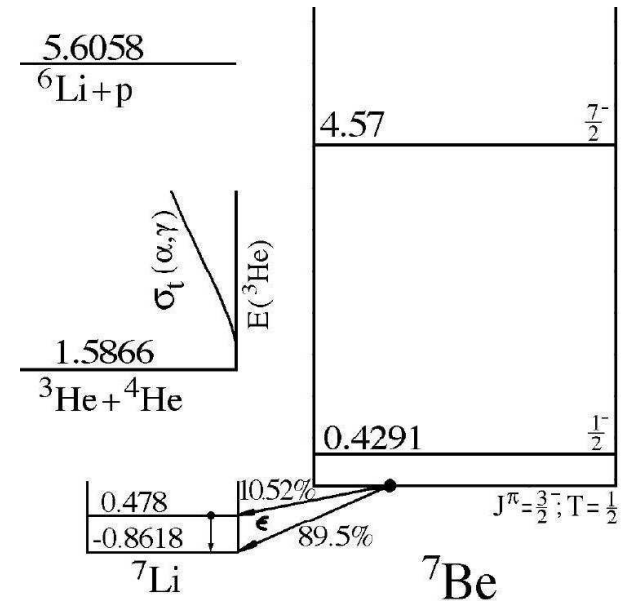
Many-Body Method:

Fermionic Molecular Dynamics

- Internal region: VAP configurations with radius constraint
- External region: Brink-type Cluster configurations
- Matching to Coulomb solutions: Microscopic R -matrix method

Results:

- ${}^7\text{Be}$ Bound States and Scattering Phase Shifts
- Astrophysical S -Factor



Potential models

- ${}^4\text{He}$ and ${}^3\text{He}$ are considered as point-like particles
- interacting via an effective nucleus-nucleus potential fitted to bound state properties and phase shifts

Microscopic Cluster Models

- antisymmetrized wave function built with ${}^4\text{He}$ and ${}^3\text{He}$ clusters
- polarization effects sometimes included by adding other channels like ${}^6\text{Li}$ plus proton
- interacting via an effective nucleon-nucleon potential, adjusted to describe bound state properties and phase shifts

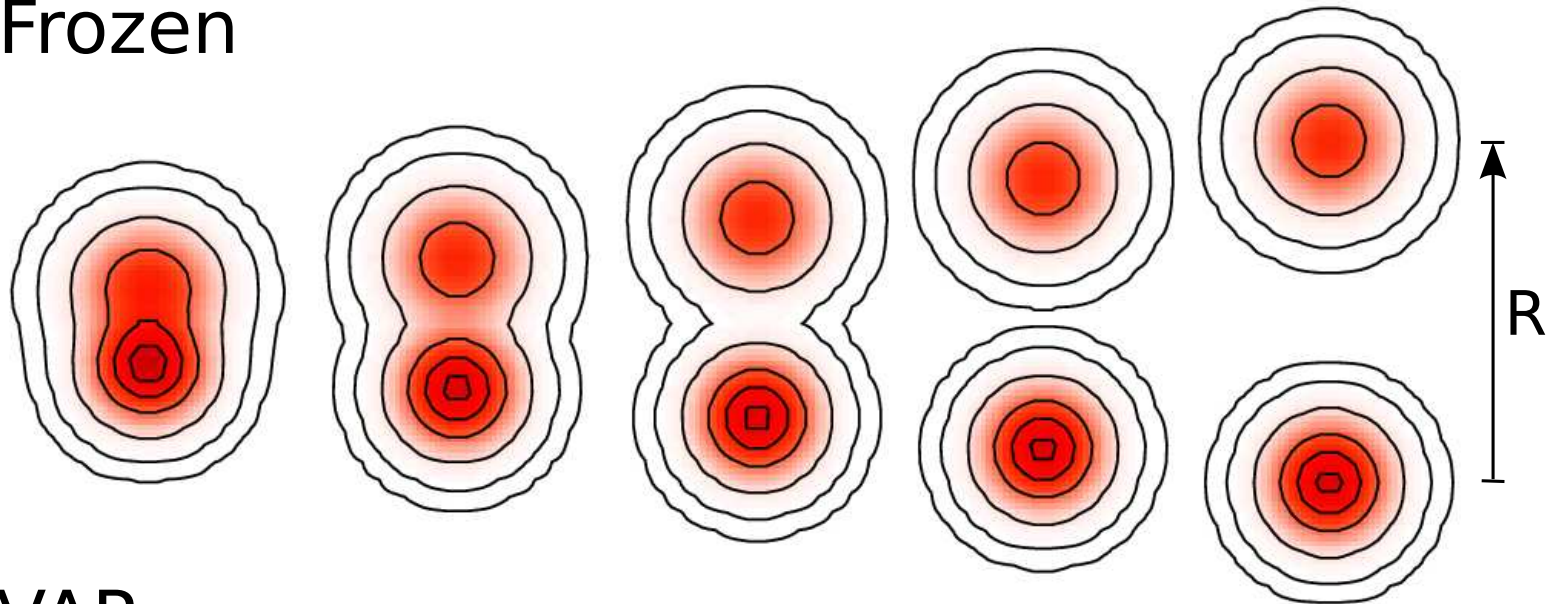
Fermionic Molecular Dynamics

- antisymmetrized wave function built with ${}^4\text{He}$ and ${}^3\text{He}$ FMD clusters
- FMD wave functions obtained in variation after angular momentum projection on $1/2^-$, $3/2^-$, $5/2^-$, $7/2^-$ and $1/2^+$, $3/2^+$ and $5/2^+$ with radius constraint in the interaction region to include polarization effects
- interacting via realistic UCOM interaction that reproduces the nucleon-nucleon phase shifts

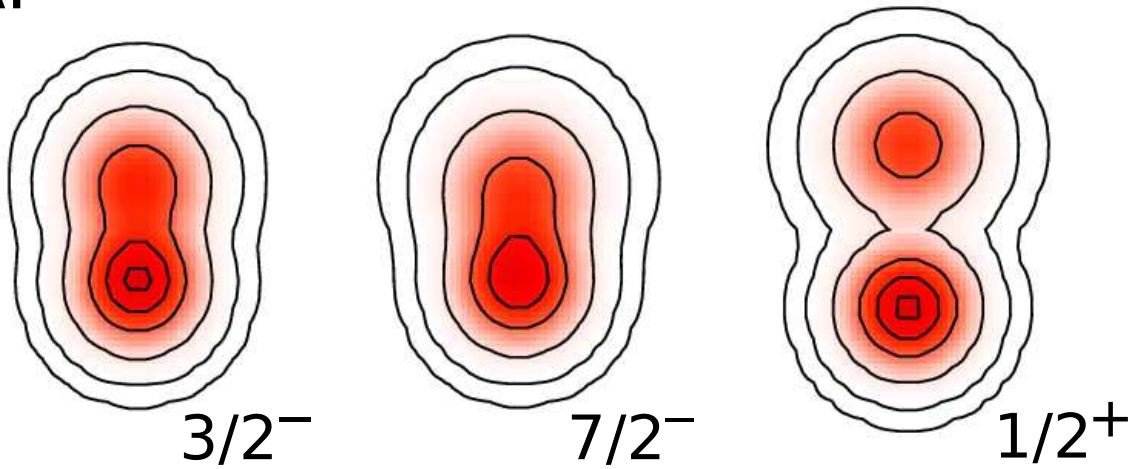
${}^3\text{He}(\alpha, \gamma){}^7\text{Be}$

Frozen and VAP Configurations

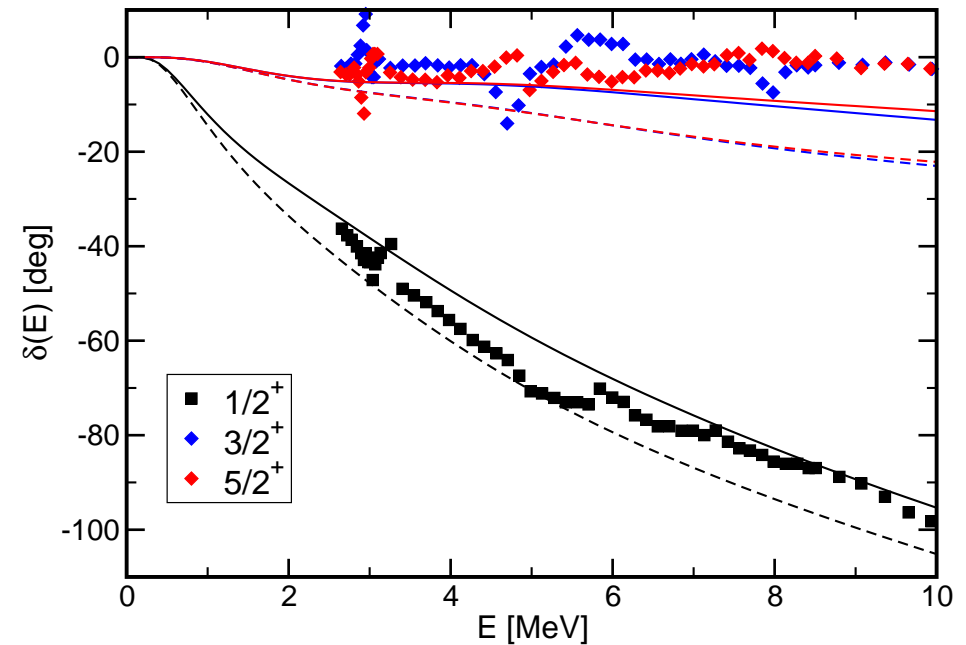
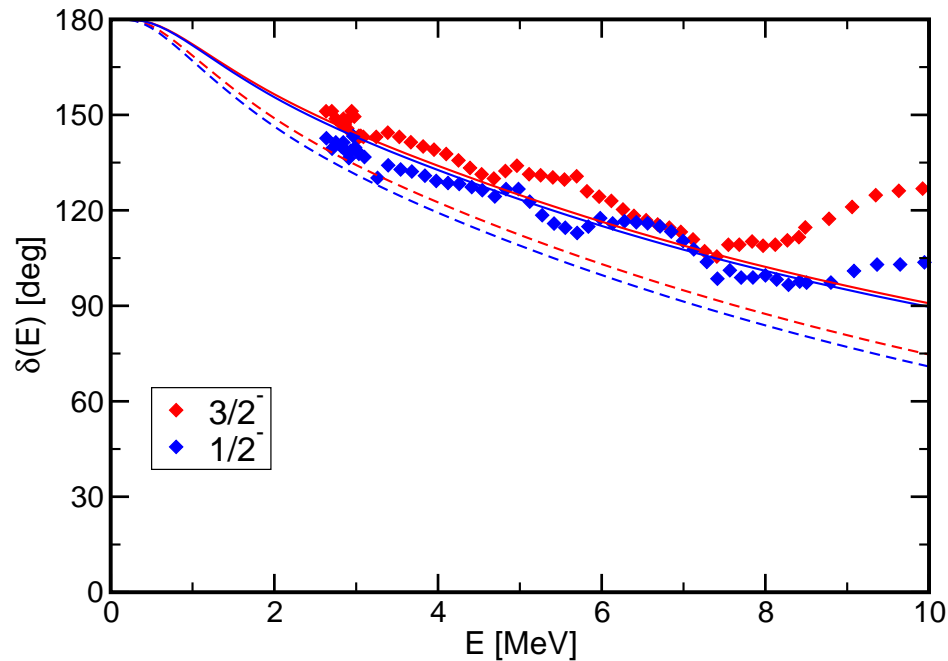
Frozen



VAP



Bound and Scattering States



dashed lines – frozen configurations only, solid lines – FMD configurations in interaction region included

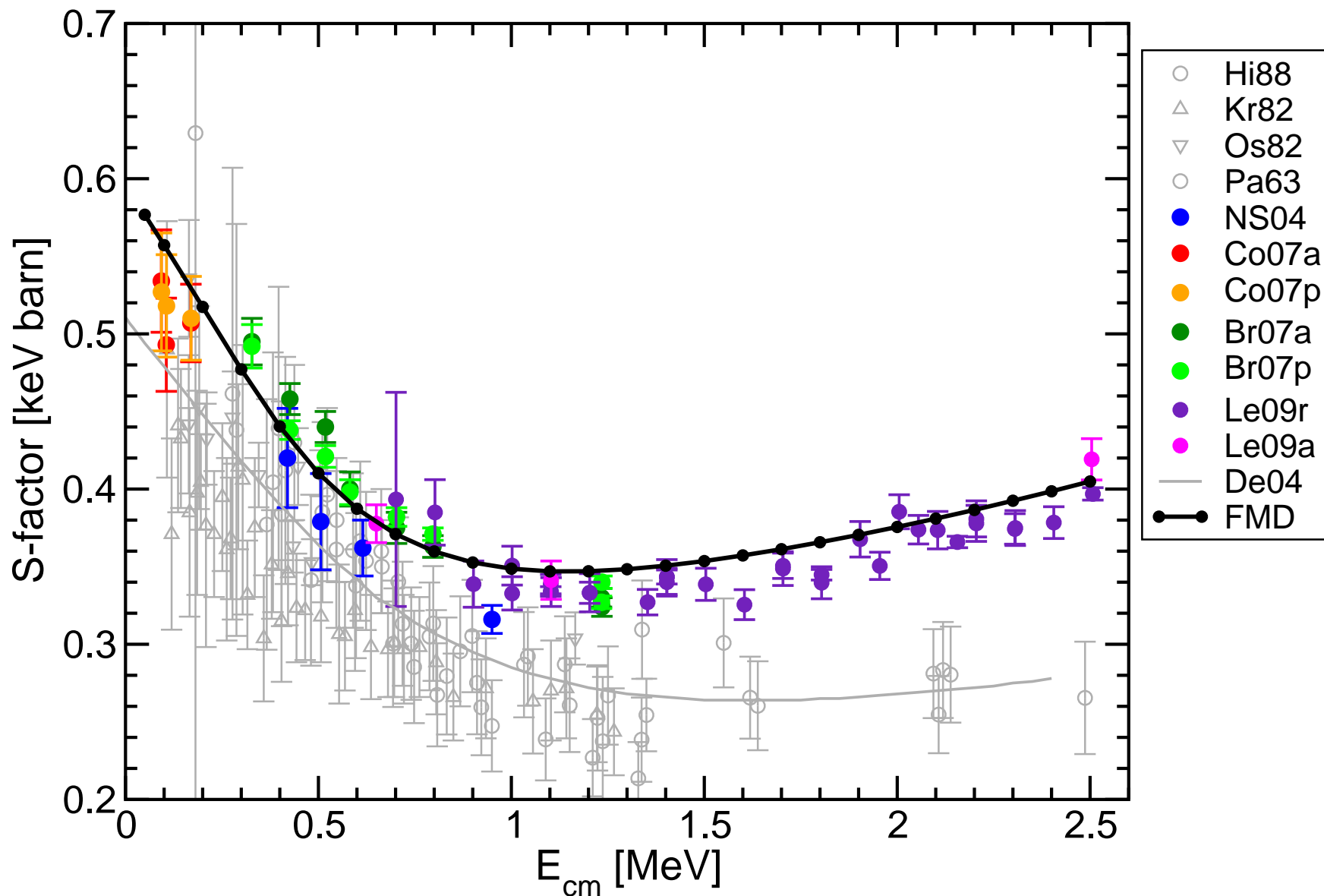
Bound states

	Experiment	FMD
$E_{3/2-}$	-1.59 MeV	-1.49 MeV
$E_{1/2-}$	-1.15 MeV	-1.31 MeV
r_{charge}	2.647(17) fm	2.67 fm

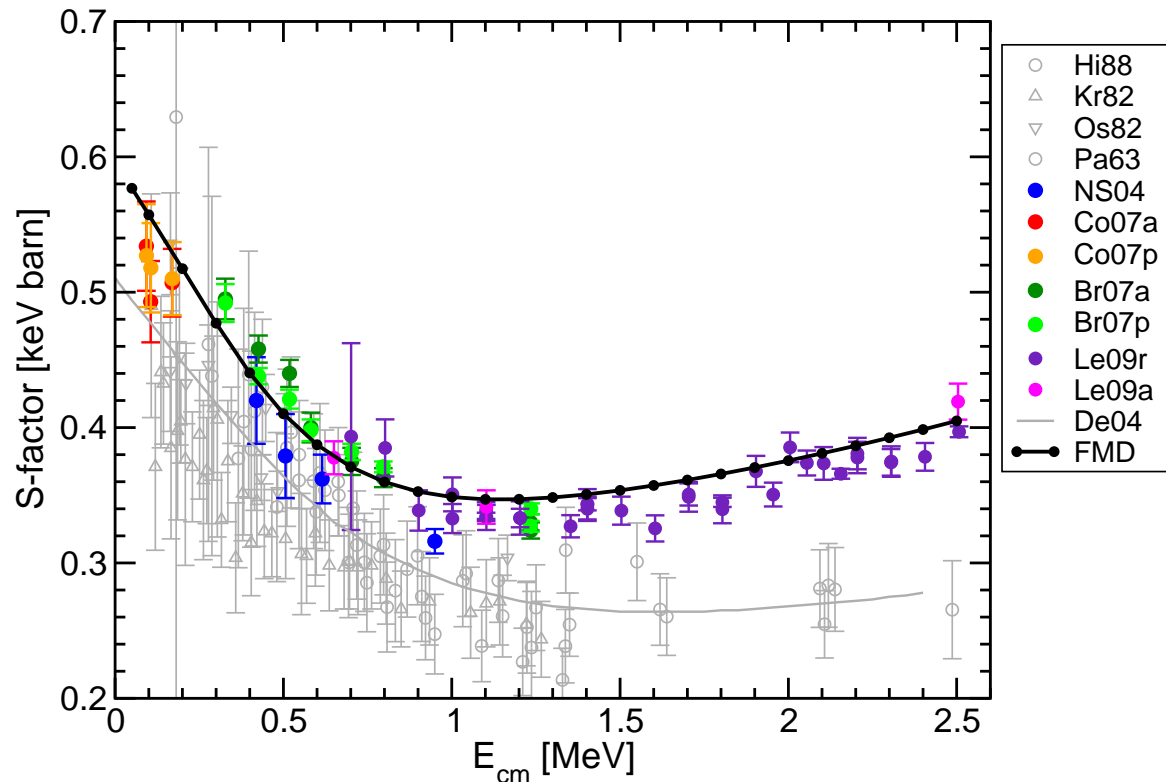
- Scattering phase shifts well described, polarization effects important
- splitting between $3/2^-$ and $1/2^-$ states too small, but centroid energy and charge radius well reproduced
- with frozen configurations only, $3/2^-$ and $1/2^-$ states are only bound by 150 and 10 keV, polarization effects are essential

$^3\text{He}(\alpha, \gamma)^7\text{Be}$

S-Factor



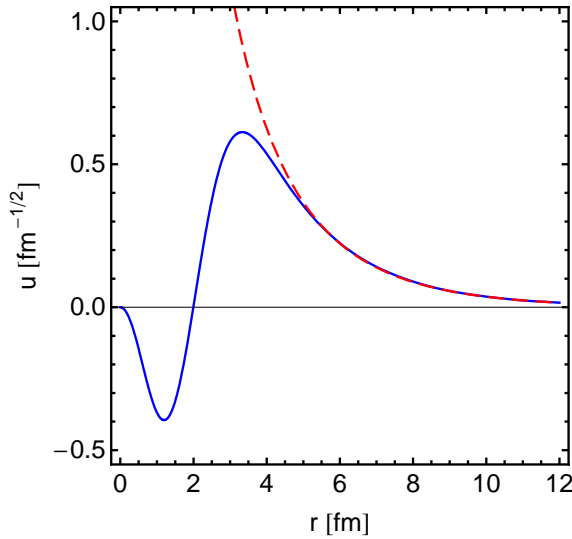
S-factor: $S(E) = \sigma(E)E \exp\{2\pi\eta\}$, $\eta = \frac{\mu Z_1 Z_2 e^2}{k}$



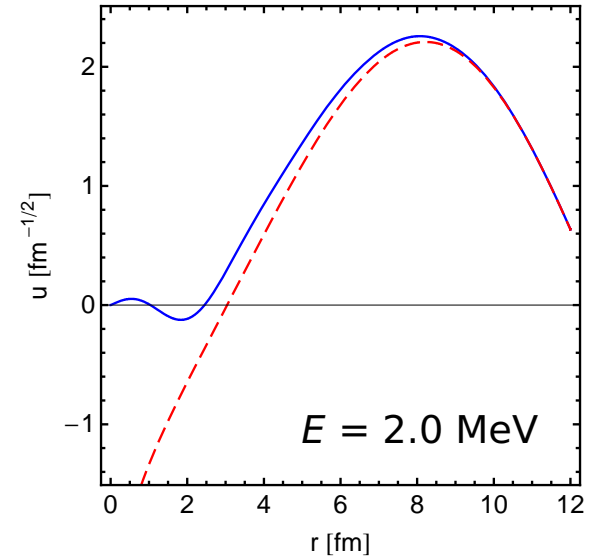
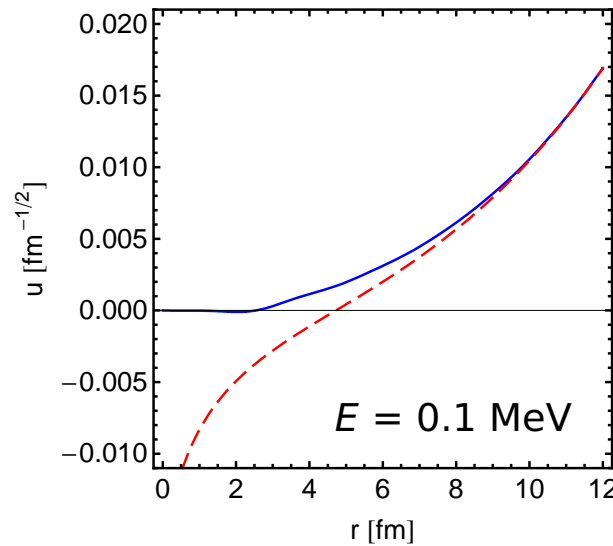
- dipole transitions from $1/2^+$, $3/2^+$, $5/2^+$ scattering states into $3/2^-$, $1/2^-$ bound states
- energy dependence and normalization of new high quality data well described
- cross section depends significantly on internal part of wave function, description as an “external” capture is too simplified
- numerics stable down to energies of 50 keV

Overlap Functions and Dipole Matrix Elements

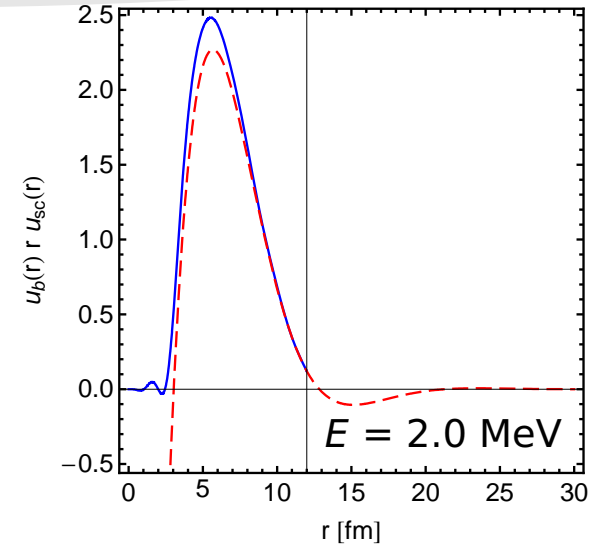
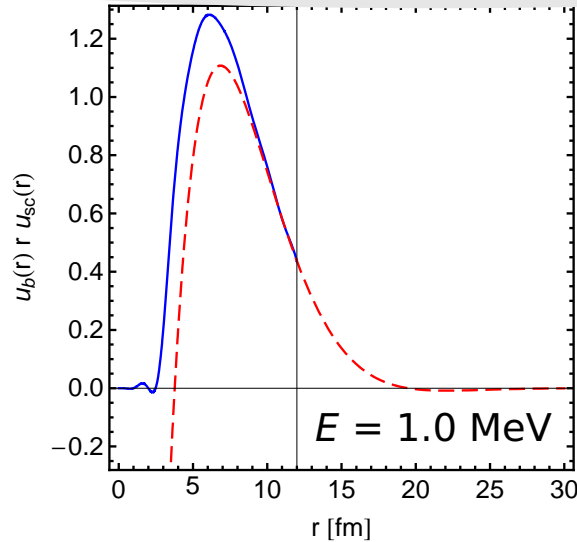
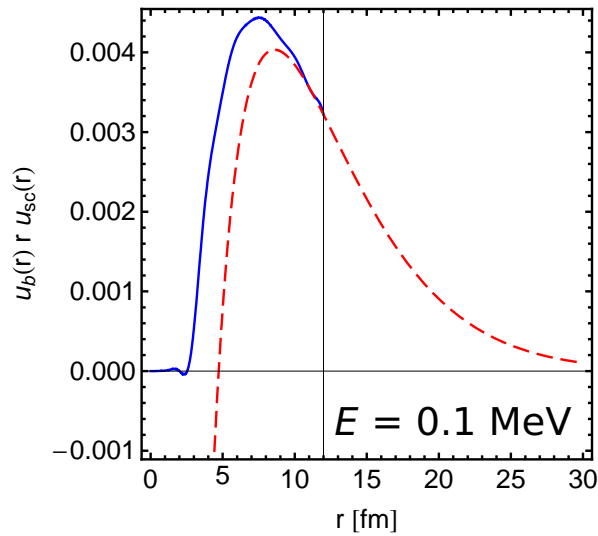
bound state



scattering states



dipole matrix elements



Advantages/Disadvantages of FMD approach

FMD vs *ab initio*

Advantages

- basis very flexible, clusters and halo structure can be described
- microscopic description of scattering
- many observables can be calculated
- intrinsic states provide an “intuitive” picture of many-body correlations

Disadvantages

- interaction has to be soft and given in operator representation
- does not provide “exact” results for given interaction, not straightforward to check convergence by “increasing model space size”

FMD vs few-body models

Advantages

- microscopic - antisymmetrization
- cluster structure appears naturally, includes polarization effects
- uses nucleon-nucleon interaction, no need for phenomenological potentials

Disadvantages

- numerical effort, “exact” calculations are not possible
- much more difficult to include boundary conditions for resonance or scattering states